



Since January 2020 Elsevier has created a COVID-19 resource centre with free information in English and Mandarin on the novel coronavirus COVID-19. The COVID-19 resource centre is hosted on Elsevier Connect, the company's public news and information website.

Elsevier hereby grants permission to make all its COVID-19-related research that is available on the COVID-19 resource centre - including this research content - immediately available in PubMed Central and other publicly funded repositories, such as the WHO COVID database with rights for unrestricted research re-use and analyses in any form or by any means with acknowledgement of the original source. These permissions are granted for free by Elsevier for as long as the COVID-19 resource centre remains active.



Original article

2-Aminopyrimidine based 4-aminoquinoline anti-plasmodial agents. Synthesis, biological activity, structure–activity relationship and mode of action studies

Kamaljit Singh^{a,*}, Hardeep Kaur^a, Kelly Chibale^b, Jan Balzarini^c, Susan Little^d, Prasad V. Bharatam^e^aOrganic Synthesis Laboratory, Department of Applied Chemical Sciences and Technology, Guru Nanak Dev University, Amritsar 143005, India^bDepartment of Chemistry and Institute of Infectious Disease and Molecular Medicine, University of Cape Town, Rondebosch 701, South Africa^cRega Institute for Medical Research, Katholieke University Leuven, 10 Minderbroedersstraat, B-3000 Leuven, Belgium^dFaculty of Infectious and Tropical Diseases, London School of Hygiene and Tropical Medicine, Keppel Street, London WC1E 7HT, UK^eDepartment of Medicinal Chemistry, National Institute of Pharmaceutical Education and Research, S.A.S Nagar 160062, India

ARTICLE INFO

Article history:

Received 1 February 2012

Received in revised form

2 March 2012

Accepted 2 March 2012

Available online 13 March 2012

Keywords:

2-Aminopyrimidine

4-Aminoquinolines

DHFR inhibitor

CT DNA interaction

DHPM

ABSTRACT

2-Aminopyrimidine based 4-aminoquinolines were synthesized using an efficacious protocol. Some of the compounds showed *in vitro* anti-plasmodial activity against drug-sensitive CQ^S (3D7) and drug-resistant CQ^R (K1) strains of *Plasmodium falciparum* in the nM range. In particular, 5-isopropoxy carbonyl-6-methyl-4-(2-nitrophenyl)-2-[(7-chloroquinolin-4-ylamino)butylamino] pyrimidine depicted the lowest IC₅₀ (3.6 nM) value (56-fold less than CQ) against CQ^R strain. Structure–activity profile and binding with heme, μ -oxo-heme have been studied. Binding assays with DNA revealed better binding with target parasite type AT rich pUC18 DNA. Most compounds were somewhat cytotoxic, but especially cytostatic. Molecular docking analysis with *Pf* DHFR allowed identification of stabilizing interactions.

© 2012 Elsevier Masson SAS. All rights reserved.

1. Introduction

Faced with the challenges of drug resistance, poor health systems, lack of affordable, safe and convenient treatment options, efficient treatment of malaria, one of the most devastating parasitic diseases, represents an unmet medical need. Malaria is a major public health concern in more than 90 countries inhabited by more than 2.4 billion people – 40% of the world's population and is responsible for almost 1 million deaths every year [1]. The majority of malaria victims in developing countries are pregnant women or children under the age of five, possessing little or no immunological protection. The disease is estimated to result in ~250 million new annual infections worldwide. Though the majority of the cases and approximately 90% of the malaria deaths are found in sub-Saharan Africa, the disease is now increasing in Asia and Latin America. Malaria is caused by protozoan parasites of the genus *Plasmodium* that infects and destroys red blood cells eventually leading to death, if untreated. The persistent threat of emergence of multidrug

resistant *Plasmodium falciparum*, universal chloroquine resistance [2,3], suspected resistance to artemisinins [4,5], and lack of effective, appropriate and affordable treatment options have given a new impetus to the research leading to broadening of the range of therapeutic targets. Thus, creating a new armamentarium of drugs with promising antimalarial activity coupled with understanding of their mode of action may lead to the development of a new generation of treatments both for malaria control and eradication.

The common feature of the drugs based on quinine **1** is the presence of a quinoline unit, usually a 7-chloroquinoline (chloroquine **2** and amodiaquine **3**, Chart 1), and are known to cause parasite death by blocking the polymerization of the toxic heme, into an insoluble and non-toxic pigment, hemozoin, resulting in cell lysis and parasite cell autodigestion [6–8]. The mode of action of 2,4-diaminopyrimidine based drugs, typified by pyrimethamine **4** [9] and the lead compound WR99210 **5** [10] is through the inhibition of *P. falciparum* Dihydrofolate reductase (*Pf* DHFR) enzyme, required for the biosynthesis of tetrahydrofolate involved in the biotransformation of thymidylate synthase-catalysed deoxyuridylate to deoxythymidylate (dUMP → dTMP), through a methyl group transfer reaction during DNA biosynthesis [11–16]. In addition, a number of polyamines inhibit ornithine decarboxylase activity in *P. falciparum* through binding with plasmodial DNA

* Corresponding author. Tel.: +91 183 2258853; fax: +91 183 2258819, +91 183 2258820.

E-mail address: kamaljit19in@yahoo.co.in (K. Singh).

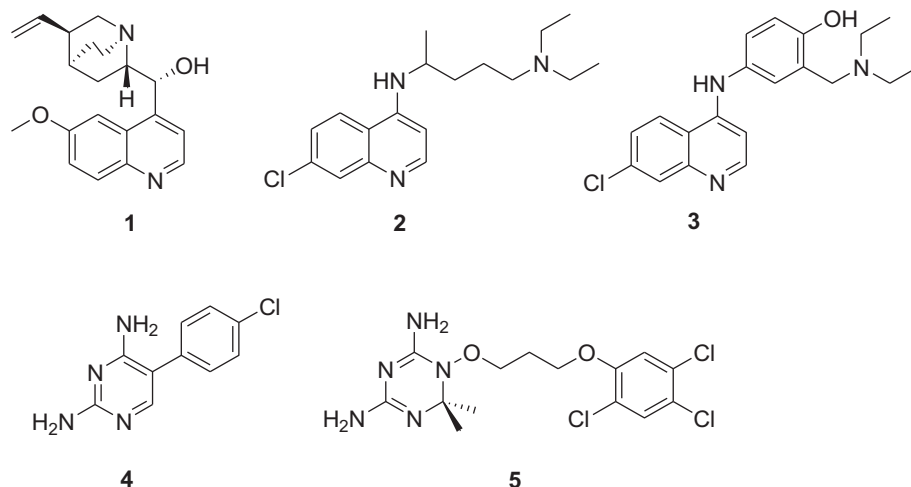


Chart 1. Antimalarial agents: quinine (1), chloroquine (2), amodiaquine (3), pyrimethamine (4) and WR99210 (5).

[17,18]. Recently, investigations in hybrid antimalarial agents, combining 4-aminoquinoline with other pharmacophore having antimalarial activity have been found to be less prone to resistance to parasite and has thus offered an effective means to overcome the problem of drug resistance.

We envisaged that linking 7-chloro-4-aminoquinoline unit, critical for antimalarial activity through a diversely functionalized lateral side chain with other antimalarial moiety such as aminopyrimidine, might furnish *conjugate hybrids* [19] capable of showing useful antimalarial activity. In this communication, we report synthesis of a set of compounds that possess basic, hydrophobic as well as hydrogen bonding substituents, required for targeting either or both heme as well as DNA, thus providing new antimalarial agents active against chloroquine resistant strains of *P. falciparum*. We have evaluated their anti-plasmodial activity, cytotoxicity and cytostatic activity, binding studies with DNA and heme (monomeric as well as μ -oxo dimeric) using UV–visible, fluorescence spectrophotometry as well as NMR analysis.

2. Chemistry

Compounds **10a–s** were synthesized as outlined in **Scheme 1**, via a common intermediate **8**. 3,4-Dihydropyrimidin-2(1H)-ones **6** were prepared through HCl-catalyzed Biginelli condensation of appropriate aldehyde (R^3CHO), alkylacetoacetate ($R^2CH_2COOR^1$) and urea [20]. Dehydrogenation of **6** using pyridinium chlorochromate in DCM furnished pyrimidinones **7** [21]. Refluxing **7** with $POCl_3$ yielded **8** which upon nucleophilic substitution reaction with appropriate 4-amino-7-chloroquinoline **9** gave **10a–s** in

a synthetically useful manner [22]. Structures of **6–10** were established on the basis of spectral (1H NMR, ^{13}C NMR, MS, FT IR) as well as microanalytical analysis. The yields of the 2-aminopyrimidines **10** are reported in **Table 1**.

3. Results and discussion

3.1. *In vitro* anti-plasmodial activity and structure–activity relationships (SARS)

Antiplasmodial activity of pyrimidines linked to CQ as in **10** has not been described in literature albeit the related dihydropyrimidin-2(1H)-ones (DHPMs) have previously been reported [23]. Using the synthetic protocol shown in **Scheme 1** allowed considerable diversification around the pyrimidine core for conducting SAR analysis. The *in vitro* anti-plasmodial activities of **10a–s** were determined in primary and secondary screening against CQ^S and CQ^R strains of *P. falciparum*. The half maximal inhibitory concentration (IC_{50}) of **10a–s** are summarised in **Table 2** (**Fig. 1**). Evidently, the compounds have anti-plasmodial activity in the nM range and against the CQ^R strain of *P. falciparum*, in some cases activity was found to be even superior to CQ. Systematic variation of the length as well as nature of the spacer connecting the pharmacophores discerned useful trends in the anti-plasmodial activity of these analogs.

Comparing **10a–g**, bearing linear alkyl spacers, revealed an increase in the anti-plasmodial activity with increase in length of the spacer up to 4 methylene groups (**10a–10c**, **Table 2**). Further lengthening of the spacer chain length resulted in significant

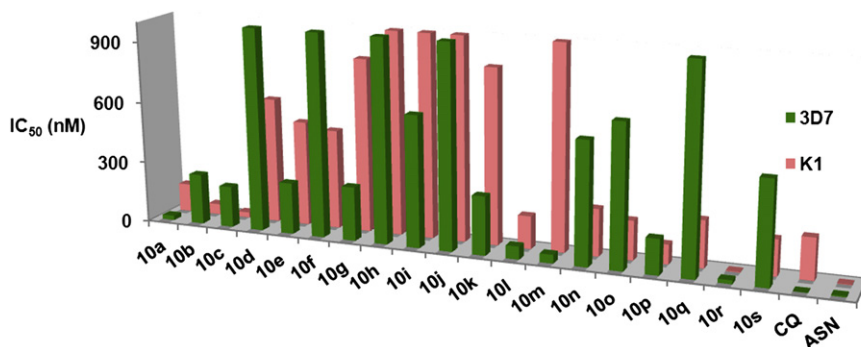


Fig. 1. Antimalarial activity of compounds **10a–s** against the CQ^S and CQ^R strains of *P. falciparum*.

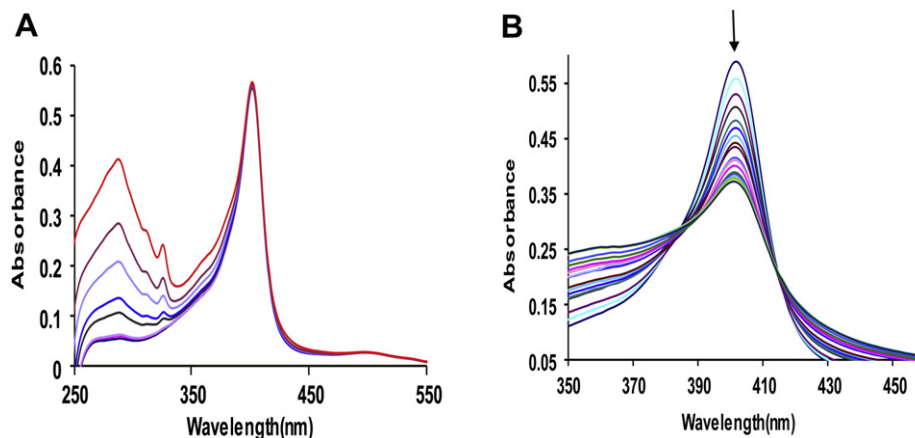


Fig. 2. Titration of **10h** (0–85.7 μM , DMSO:H₂O/4:6, v/v) (a) and **10i** (0–8.85 μM , DMSO:H₂O/4:6, v/v) (b) with heme (2.4 μM , DMSO: H₂O/4:6, v/v).

reduction in activity against both the CQ^R as well as the CQ^S strains. Replacing the C-4 phenyl group in **10c** by a methyl group to create **10m** resulted in nearly 5 times increase in anti-plasmodial activity (IC₅₀ 42.1 nM) against the CQ^S strain. In fact, compound **10m** was found (Table 2) to be the most active compound of the series, against the CQ^S strain. However, **10m** exhibited a high resistance factor (~ 39) within the series but is 3.5 times less active than CQ, against the CQ^R strain. Replacement of the ethyl ester with *iso*-propyl ester (**10n–s**), in general showed a decrease in *in vitro* anti-plasmodial activity against the CQ^S strain, although a reverse trend was observed for the CQ^R strain, especially in case of **10s**, **10p** and **10r**, where replacing C-4 phenyl by *p*-nitrophenyl (**10s**) or *o*-nitrophenyl (**10p** and **10r**) groups, in addition to incorporating an *isopropyl* ester, resulted in an increase of activity in that order, rendering **10r** as the most potent (IC₅₀ 3.6 nM, 56 times more potent than CQ, Table 2) of all these compounds. These results are in accordance with the trend observed in case of N, N-bis(7-chloroquinolin-4-yl)alkane diamines, wherein the alkyl spacer consisting of four carbon atoms showed optimum potency [24].

The better anti-plasmodial activity of phenyl-substituted pyrimidine compounds against the CQ^R strain may be attributed to optimal fitting of these compounds in the active site of *Pf*DHFR leading to a favorable conformation for π - π interaction with the heme functionality. Moreover, the introduction of a nitro substituent on the phenyl ring at the C-4 position of the pyrimidine core

results in a significant increase in anti-plasmodial activity as well as resistance against the CQ^R strain, although it has little effect on activities against the CQ^S strain (Table 2). Also, the corresponding *o*-, *m*- or *p*-nitro derivatives showed considerable variation in anti-plasmodial activity (Table 2). Comparison of compounds (**10n**, **10q**, **10s**) having an identical spacer reveals that the *p*-NO₂ substituted **10s** (IC₅₀ 175.8 nM) is more active than the *o*-/*m*-NO₂ substituted compounds **10q** and **10n**, respectively, but are less active than the unsubstituted ethyl ester analog **10b**. Further, comparison with the butyl spacer analog suggests that *o*-NO₂ phenyl derivative **10r** is more potent than the *m*-NO₂ counterpart **10o**, as well as its ethyl ester analog **10c**, against the CQ^R strain. Compound **10r** was found to be the most active compound in this series against the CQ^R strain with anti-plasmodial activity (IC₅₀ 3.6 nM), 56 times more than CQ (IC₅₀ 201.8 nM) and comparable to artesunate (IC₅₀ 2.8 nM) (Table 2).

Comparing **10j** (IC₅₀ 28096.7 nM) possessing the branched chain spacers with identical carbon linear spacer analog **10b** (IC₅₀ 52.2 nM, Table 2) led to significant decrease in activity. Thus, compound **10j** displayed a 540-fold decrease in activity compared to **10b**, against the CQ^R strain. Likewise, **10k** possessing a branched C-6 spacer depicted a decrease (IC₅₀ 860.4 nM, Table 2) in activity against linear alkyl (C-7) spacer analog **10d** (Table 2), but higher than **10j**. Comparing **10j** and **10k**, with branched chain spacers, not only was the anti-plasmodial activity of the latter against both CQ^S

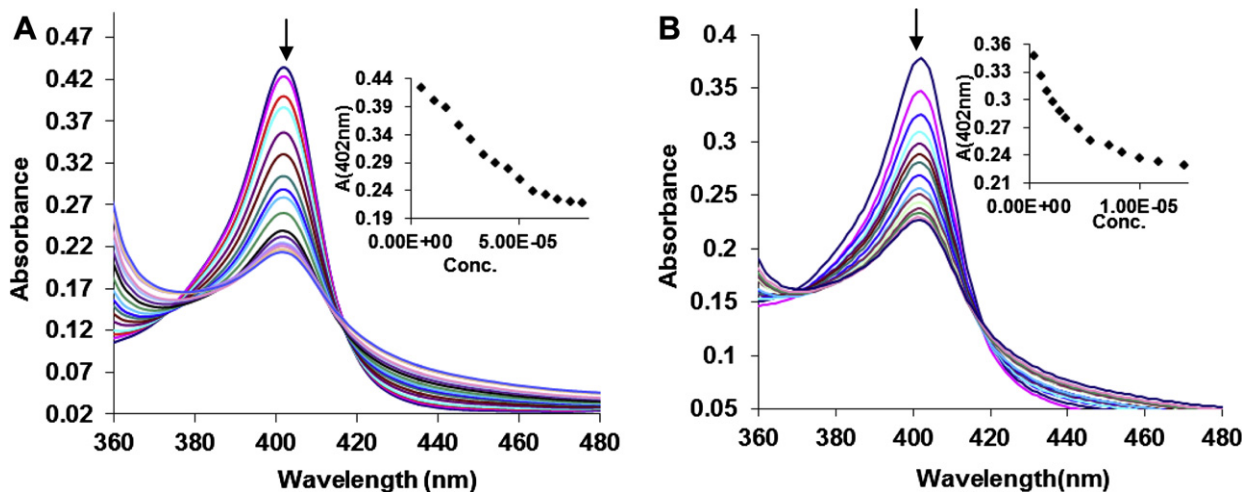


Fig. 3. Titration of **10r** (A) and **10c** (B) with monomeric heme at pH 7.5.

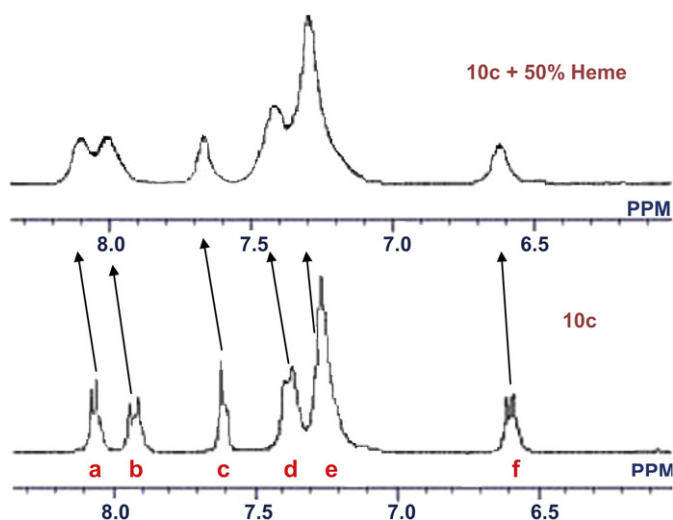


Fig. 4. The 300 MHz ^1H spectra of **10c** upon addition of heme (50 mol % in 40% $\text{DMSO-D}_2\text{O} \backslash \text{D}_2\text{SO}_4$ (10 μl)) [$\Delta\delta$ for peak: a = 0.025, b = 0.105, c = 0.052, d = 0.029, e = 0.032, f = 0.032].

and CQ^{R} strains increased, but it also showed an increased resistance factor (Table 2). The replacement of linear chain spacers with *o*- and *p*- linked aryl groups (**10h** and **10i**, respectively), led to much higher IC_{50} (Table 2) values compared to former against CQ^{R} strain, while only moderate activity was observed in case of **10i** against CQ^{S} strain. These findings could be attributed to the increased steric bulk (**10h** more than **10i**) affecting the interaction of the iron center of heme with the compounds. This has been corroborated by performing the titration of monomeric heme with both **10h** and **10i**. While the titration of heme (2.4 μM , $\text{DMSO:H}_2\text{O}/4:6$, v/v) with increasing concentration of **10h** (0–85.7 μM , $\text{DMSO:H}_2\text{O}/4:6$, v/v) revealed no change in the absorbance at 402 nm (Fig. 2a), the addition of **10i**, in a similar way showed marked gradual decrease in absorbance at 402 nm. The decrease in absorbance continued until the concentration of **10i** was 8.85 μM (Fig. 2b), representing 1:4 molar ratio of heme and **10i**. Hence, the flexibility, chain length and steric constraints of the spacer linking quinoline moiety and pyrimidine unit seem to play a role in anti-plasmodial activity of these derivatives. Although the *in vitro* activity of **10a–c**, **10p** and especially **10r** (IC_{50} 3.6 nM) was superior to CQ (IC_{50} 201.8 nM) against the CQ^{R} strain, these compounds suffer from high ClogP values (Table 2), which are suggestive of the fact that these possess limited aqueous solubility, which in fact is not a serious limitation in view of recent advancements in formulation methods.

3.2. Cytotoxicity and antiviral activity

Antiviral activity of the compounds **10a–c**, **10l–n**, **10p** and **10r**, which were active against the CQ^{R} strain was also evaluated against (i) parainfluenza-3 virus, reovirus-1, Sindbis virus, Coxsackie virus B4, Punta Toro virus in vero cell cultures, (ii) herpes simplex virus –1 (HSV-1; KOS), herpes simplex virus-2 (HSV-2; G), vaccinia virus, vesicular stomatitis virus, herpes simplex virus-1 (TK⁻KOS ACV^R), cytomegalovirus, varicella-zoster virus in HEL cell cultures, (iii) vesicular stomatitis virus, coxsackie virus B4, respiratory syncytial virus in HeLa cell cultures, (iv) influenza A virus (H1N1 and H3N2) and influenza B virus in MDCK cell cultures and (v) feline corona virus (FIPV) and feline herpes virus activity in CRFK cell cultures (SI Tables S1–S7). Unfortunately, no significant antiviral activity was noted at subtoxic concentrations. Most compounds were somewhat cytotoxic to the different cell lines (confluent non-proliferating cultures), but especially cytostatic against proliferating (Vero/MDCK/CRFK) cell cultures. Chloroquine has been shown to inhibit HIV through blockade of viral entry *via* inhibition of endosomal acidification [25,26]. Compounds **10a–c**, **l–n**, **p**, **r** were also tested against HIV-1 as well as HIV-2 (SI Table S8) in human T-lymphocyte (CEM) cell cultures. However, none of the compounds were active at subtoxic concentrations.

Generally, the compounds exhibit a relatively high cytostatic activity but displayed a fairly safe selectivity index (except **10m** and **10n**) (Table 2) in the range of 10.04–638 against MDCK cell cultures. The most active compound **10r** with an IC_{50} value of 3.6 nM against CQ^{R} strain exhibited a highest selectivity index ($\text{SI} = 638$), **10l** with an IC_{50} value of 160.8 nM against CQ^{R} strain exhibited a high selectivity index (361.9). However, **10m** having an IC_{50} value of 1659.8 nM was most toxic with a selectivity index of 0.48.

3.3. Insight into the mode of action and $\text{Fe(III)PPIX-10c/10r}$ association constants

The plausible mechanism of *in vitro* anti-plasmodial action against CQ^{R} strain has been investigated for **10c** and **10r**, found to be most potent of the series of the compounds reported herein (IC_{50} 26.1 nM, **10c** and IC_{50} 3.6 nM, **10r**). These compounds are also expected to bind to heme [Fe(III)PPIX] (hydroxo or aqua complex of ferriprotoporphyrin IX) in solution and inhibit aggregation to β -hematin, in much the same way as CQ itself. The higher ClogP values (Table 2) of these compounds being higher than CQ necessitated the use of aqueous DMSO as solvent. Also in 40% aqueous DMSO solution, heme is expected to be monomeric, while in purely aqueous solutions, it exists in aggregated form. Further, it is known that CQ binds to heme dimer (μ -oxo heme) *in vitro* and can also

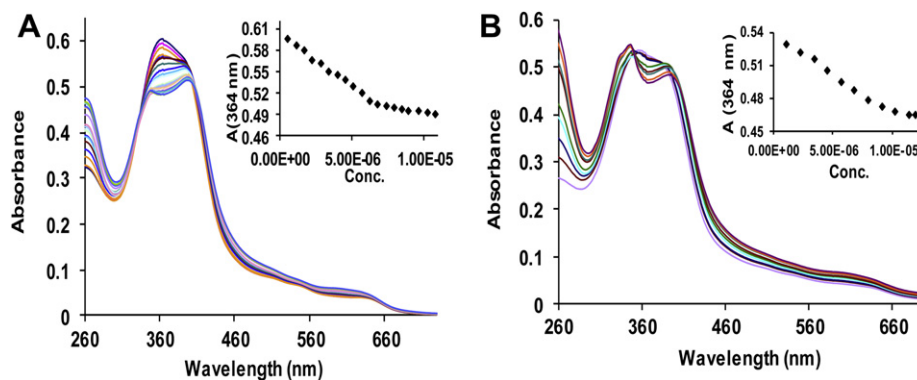


Fig. 5. Titration spectra of **10r** (A) and **10c** (B) with μ -oxo heme at pH 5.8.

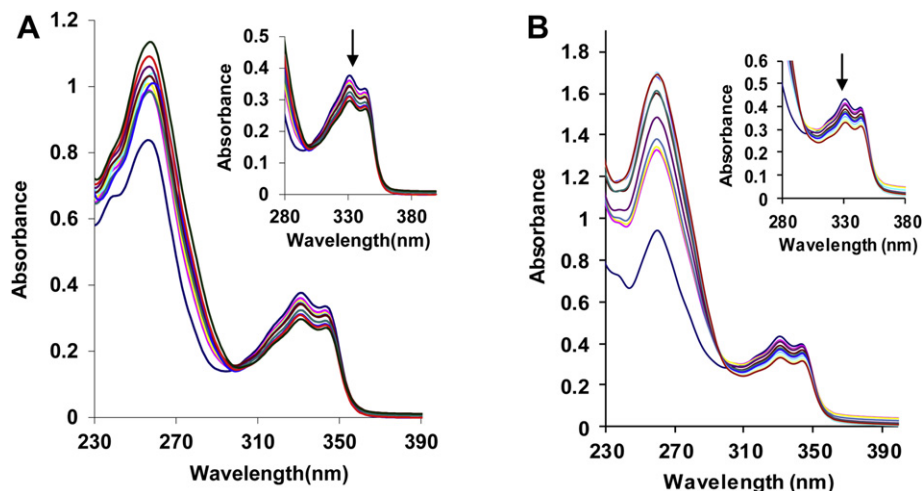


Fig. 6. Absorption spectra of **10c** (A) and **10r** (B) in the presence of different CT DNA concentration inset show zoom between 280 and 380 nm.

inhibit the formation of β -hematin, the *in vitro* analog of hemozoin [27–30]. Therefore the binding assay was also extended to heme dimer also. The interaction of **10c** and **10r** with monomeric heme was followed by spectrophotometric titration at pH 7.4 and 5.6 (the approximate pH of food vacuole), as described previously [31]. The spectral changes (Fig. 3A, SI Figure S1), upon addition of increasing amounts (0–70 μ M) of **10r** to a solution of heme (2.4 μ M, HEPES buffer pH 7.4) showed substantial decrease of intensity of the Fe(III) PPIX Soret band at 402 nm with no shift in the absorption maximum. The longer wavelength Q-bands (494 and 537 nm) of the metalloporphyrin also decrease in intensity (SI Figure S2) [32]. A sharp isosbestic point was observed at 416 nm (pH 7.4) and at 412 nm (pH 5.6). The association constants for the complexes formed between monomeric Fe (III) PPIX and **10r** at pH 7.5 and 5.6 were calculated from titration data and are presented in Table 3.

The association constant of **10c** (Fig. 2A) is found to be greater ($\log K$ 6.018) than **10r** ($\log K$ 5.078). Decrease in the apparent pH from 7.5 to 5.6 caused a fairly modest decrease in $\log K$ values of both **10c** and **10r**, indicating a strong binding to heme even at acidic pH. The binding of **10c** and **10r** was also assessed from their ^1H NMR titration with heme. Thus, while ^1H NMR spectrum of **10r** depicted considerable broadening of signals under the conditions (40% DMSO- d_6 in D_2O) of recording and was inconclusive, the variation in the chemical shift in signals corresponding to quinoline unit of **10c** were clear (Fig. 4), upon addition of heme.

A 1:1 stoichiometry of the most stable complexes of both **10r** and **10c** with monomeric heme at pH 7.5 and 5.6 was deduced from the Job's plot (SI Figure S3) [33,34]. The absorbance at 402 nm got to maximum when mole fraction of **10r** approached 0.5. This is in good agreement with the association constant ($\log K$) values corresponding to the most stable 1:1:heme: **10r** species present in solution, obtained by fitting the titration data in Hyp Spec - a non-linear least square fitting programme. The measured $\log K$ values for both **10r** and **10c** (Table 3) are also in good agreement with the values reported in literature for CQ [32,35,36]. Thus, the formation of synthetic Fe(III)PPIX-**10r** complex, as demonstrated above is suggestive of inhibition of formation of β -hematin and presumably results in anti-plasmodial activity of these compounds in a fashion similar to that of CQ.

Titration of constant concentrations of heme in aqueous NaOH solution at the physiological pH 5.8 of *Plasmodial* food vacuole [35] allowed understanding of the interaction of **10r** and **10c** with μ -oxo heme. With addition of increasing amount of **10r** to the solution of μ -oxo heme, the absorbance of Soret band (362 nm) decreased appreciably with significant red shift (362–405 nm, Fig. 5A). The association constants and stoichiometry for both **10r** and **10c** were determined from titration data and are presented in Table 3. The calculated association constant of **10r** ($\log K$ 6.31) is greater than **10c** ($\log K$ 6.09) and corresponds to 1:1 stoichiometry of the **10r**: μ -oxo heme complex. The comparison of association constants of **10r**

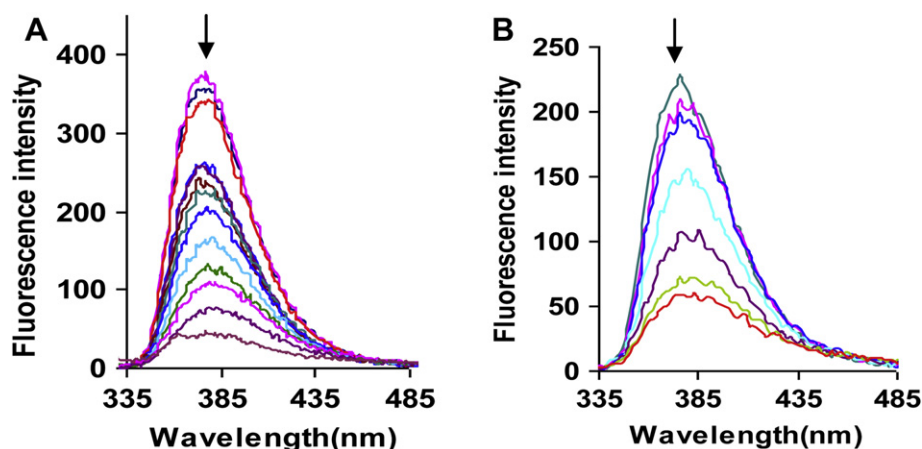


Fig. 7. Fluorescence emission spectra of **10r** at 380 nm in the presence of increasing concentrations of CT DNA (A) and pUC18 DNA (B).

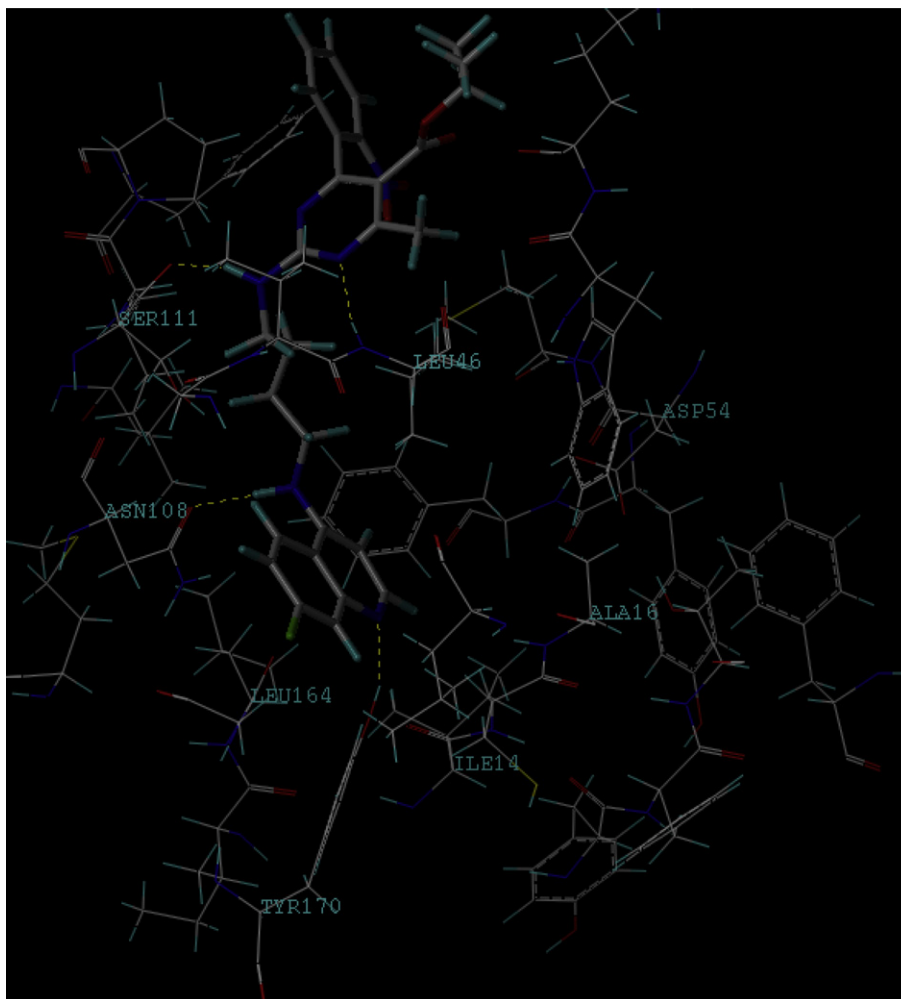


Fig. 8. The interactions of the substrate **10r** in the active site cavity of the enzyme *Pf*DHFR. The hydrogen bonding interactions with the amino acids Ile14, Leu46, Asn108, Ser111 and Tyr170 are shown with dotted yellow lines.

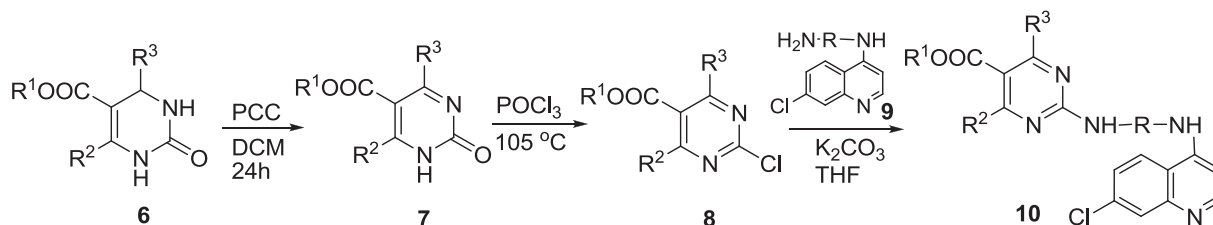
and **10c** for monomeric and μ -oxo heme reveals that both compounds bind strongly with μ -oxo heme than monomeric heme and inhibit hemozoin formation by blocking the growing face of heme resulting in the observed anti-plasmodial activity. Further, all the compounds were also screened for *in vitro* inhibition of β -hematin formation using β -hematin inhibitory assay in order to further confirm their mechanism of action based on interference with the heme detoxification process [37,38].

As shown in Table 4, there is a general correlation between anti-plasmodial activity and inhibition of β -hematin formation, but the same generalisation does not hold for compound **10h**, as, in spite of having 100% β -hematin inhibition (Table 4), it is one of the least active (IC_{50} 27320.9 nM, CQ^R and IC_{50} 14828.3 nM, CQ^S) compounds of the series. However, it must be noted that anti-plasmodial activity not only depends upon the β -hematin inhibition but also on

other factors such as degree of accumulation of drug in food vacuole. Further, **10r** showed dose dependent inhibition of β -hematin formation (SI Figure S4) with an IC_{50} value lower than those reported for CQ and quinine, thus demonstrating a better ability to interact with Fe(III)PPIX. Overall, these compounds showed strong β -hematin inhibition which seems to be their preferred mode of action.

3.4. DNA binding affinity

DNA binding has been considered previously as one of the possible mechanisms for anti-plasmodial activity and has been studied using spectrophotometry [39], spectrofluorimetry [40], DNA melting [41], viscometry [42] etc. Recently, some 4-aminoquinoline derivatives have been shown to interact with



Scheme 1. Synthesis of **10**.

Table 1
Synthesis of 2-aminopyrimidines **10**.

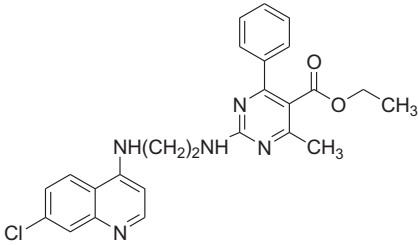
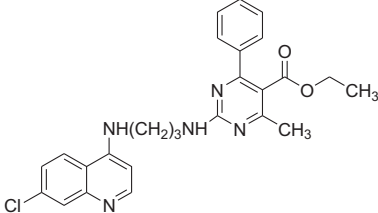
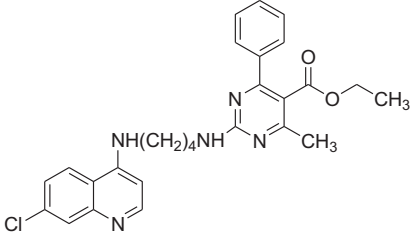
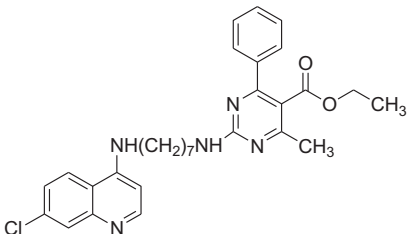
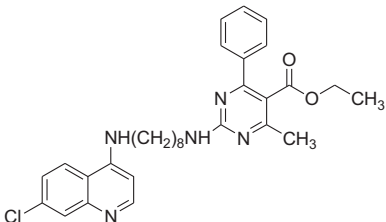
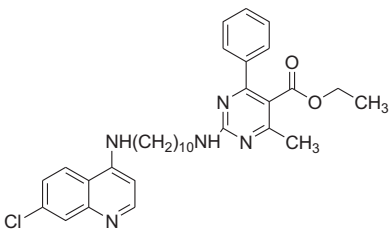
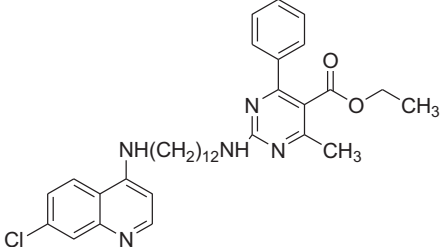
S. No.	Compound ^a	Structure	Yield (%)
1.	10a		89
2.	10b		84
3.	10c		77
4.	10d		67
5.	10e		72
6.	10f		64
7.	10g		65

Table 1 (continued)

S. No.	Compound ^a	Structure	Yield (%)
8.	10h ^b		53
9.	10i ^b		57
10.	10j		58
11.	10k		55
12.	10l		92
13.	10m		90
14.	10n		71

(continued on next page)

Table 1 (continued)

S. No.	Compound ^a	Structure	Yield (%)
15.	10o		78
16.	10p		66
17.	10q		73
18.	10r		85
19.	10s		82

^a THF, K₂CO₃, rt.^b MeCN, K₂CO₃, 80 °C.

DNA [37] presumably through ionic interactions between phosphate groups of DNA and protonated amine sites resulting in stabilization of the helical configuration of DNA against thermal denaturation [41,43]. Additionally, interactions between aromatic nucleuses of the drug with nucleotide bases might also contribute. Binding of the plasmid DNA with CQ resulted in the elevation of the thermal melting temperature (T_m) of DNA in addition to other effects [44–47]. We therefore investigated the binding of the most active of the series, **10c** and **10r** toward GC rich Calf Thymus DNA (CT DNA) as well as AT rich pUC18 DNA through stepwise addition

of small increments of DNA to a solution the compounds at constant concentration as well as physiological pH (Fig. 6A and B). A progressive decrease in the characteristic quinoline ring absorptions at 320 and 340 nm attributable to the intercalation of the quinoline into DNA was indicated.

The isosbestic point at 350 nm indicated that the spectra of limiting systems (i.e. the spectra of free and completely bound drug) intersect and permitted the selection of a single wavelength for study of complex formation. The binding constant ($\log K$: **10c** 4.67 and **10r** 3.39) was calculated from Benesi–Hildebrand

Table 2*In vitro* anti-plasmodial activity, cytotoxicity, resistance factor and selectivity index of compounds **10a-s**.

Compound	IC ₅₀ (nM)		Resistance factor ^e	ClogP ^f	Cytotoxicity (μM) ^g		Selectivity index ^j
	CQ ^S (3D7) ^{a,b}	CQ ^R (K1) ^{c,d}			CC ₅₀ ^h	MIC ⁱ	
10a	21.7	139.3	6.43	6.83	1.4	0.8	10.04
10b	247.5	52.2	0.210	6.82	0.8	0.8	15.33
10c	202.3	26.1	0.129	7.35	0.9	0.8	34.41
10d	1134.9	617.7 ^b	0.544	8.94	–	–	–
10e	252.2	516.4	2.047	9.47	–	–	–
10f	1776.8	487.7	0.2744	10.53	–	–	–
10g	264.8	853.7	3.22	11.58	–	–	–
10h	14828.3	27320.9	1.842	8.81	–	–	–
10i	644.4	6186.4 ^b	9.600	8.80	–	–	–
10j	15888.5	28096.7	1.7683	5.31	–	–	–
10k	286.7	860.4 ^b	3.00	8.28	–	–	–
10l	63.1	160.8	2.5480	5.64	58.2	20	361.89
10m	42.1	1659.8 ^b	39.422	5.75	0.8	4	0.48
10n	598.7	230.5 ^b	0.385	7.30	0.5	0.8	2.1
10o	697.2	192.1	0.2756	7.30	–	–	–
10p	172.9	96.0	0.5555	6.89	2.2	≥0.8	22.90
10q	1955.1	229.3	0.1173	7.30	–	–	–
10r	18.2	3.6	0.2	7.30	2.3	4.0	638
10s	499.9	175.8	0.3518	7.30	–	–	–
2	1.4	201.8	140.39	5.1	–	–	–
Artesunate	5.3	2.8	0.5418	1.06	–	–	–

^a CQ sensitive strain.^b primary screening.^c CQ resistant strain.^d secondary screening.^e calculated by dividing IC₅₀ values of PFK1 by PF3D7.^f calculated from Chem draw Ultra 11.0.^g determined on Madin Darby canine kidney (MDCK) cells.^h 50% cytotoxic concentration, as determined by measuring the cell viability with the colorimetric formazan-based MTS assay (reference drugs used: Oseltamivir carboxylate CC₅₀/MIC >100, Ribavirin CC₅₀/MIC >100, Amantadine CC₅₀/MIC >200 and Rimantadine CC₅₀/MIC >200).ⁱ minimum compound concentration that causes a microscopically detectable alteration of normal cell morphology.^j Selectivity Index (S.I.) is calculated as CC₅₀/IC₅₀ (K1 Strain) ratio.

equation [48] and suggested strong interaction with CT DNA. Comparison of binding constants reveals that **10c** binds 20 times more strongly with CT DNA than **10r**.

Altering the DNA base composition to see its effect on the drug binding, we studied the interaction of **10r** with GC rich CT DNA by fluorometric titration. The emission band at 380 nm of **10r** (Fig. 7), decreases in intensity with increasing concentration and eventually gets completely quenched. The binding constant (log *K*) calculated from the fluorescence data is 4.67. Similar titration with AT rich pUC18 DNA (log *K* = 5.27) revealed higher affinity of **10r** toward AT rich pUC18 DNA unlike CQ which is known to interact strongly with GC rich DNA [46]. The strong interaction of the pyrimidine analog with AT rich pUC18 DNA further suggests that these compounds might target parasite DNA which has unusually a high AT content [47] in addition to β-hematin inhibition. The binding of ligand to nucleic acid of DNA (especially AT rich DNA) may possibly induce conformational changes depending upon the strength and mode of its interaction with nucleic acids and thus result in increase in the thermal denaturation temperature, as observed for CQ.

Table 3Binding constant (log *K*) For **10r** and **10c**.

Compound	Monomeric heme		μ-oxo heme	CT DNA log <i>K</i> ± σ
	log <i>K</i> ± σ		log <i>K</i> ± σ	
	pH 5.6	pH 7.5	pH 5.8	
10r ^a	4.97 ± 0.005	5.075 ± 0.01	6.31 ± 0.01	3.39 ± 0.02
10c ^a	5.284 ± 0.01	6.018 ± 0.008	6.09 ± 0.02	4.67 ± 0.04
CQ	4.82	5.2 ^b	5.6 ^c	ND
Stoichiometry	1:1		1:1	ND

^a Calculated from Hyp Spec.^b Refer to text Ref. [35].^c Refer to text Ref. [36].

Groove binding or electrostatic binding of the phosphate backbone of DNA gives rise to small changes in thermal denaturation temperature compared to the intercalation pathway due to stabilization of Watson crick base paired duplex [43,48,49,50]. In the direction of evaluating strength of interaction of **10c** and **10r** with DNA, the thermal behavior (SI Figure S5) of CT DNA in the presence of drug was evaluated. The thermal denaturation temperature of CT DNA (60 °C), in the presence of **10c** and **10r** recorded an increase in Δ*T*_m of 3 °C and 2.5 °C, respectively (SI Table S9), suggesting primary groove binding and/or partial intercalative nature of the interaction.

3.5. Molecular docking analysis

Many of the anti-plasmodial agents are known to interact with *Pf* DHFR for their anti-plasmodial activity. Especially

Table 4

β-hematin inhibitory assay.

Compound	% Inhibition ^a	Compound	% Inhibition ^a
10a	96	10l	66
10b	100	10m	100
10c	100	10n	79
10d	89	10o	92
10e	56	10p	–
10f	–	10q	89
10g	–	10r	100 (2) ^b
10h	53	10s	94
10i	100	CQ ^c	18 ^b
10j	35	Quinine ^c	324 ^b
10k	–		

^a The percentage inhibition at 1 mg/ml (highest concentration tested).^b IC₅₀ (μM).^c Refer to text Ref. [37].

pyrimethamine (Chart 1) is known to produce anti-plasmodial effect by binding to *Pf* DHFR. The best known lead compound for this inhibitory activity is WR99210 (**5**). It is worth comparing the performance of the compounds designed in this work with that of **5**, using molecular docking methods. The crystal structure (PDB id: 1J3I, a structure of wild-type *Pf* DHFR-TS complexed with WR99210, NADPH, dUMP) was considered for molecular docking analysis. After appropriately preparing the protein structure of *Pf* DHFR, docking of **5** and **10r** were carried out. Fig. 8 shows the top scoring binding pose of **10r** in the active site of *Pf* DHFR. The docking score for **10r** is -24.5 , which is much better than that of the lead compound **5** (-20.1). The origin of this improvement in docking score can be traced to the increased number of stabilizing interactions between **10r** and *Pf* DHFR, in comparison to the interactions between **5** and *Pf* DHFR. **10r** shows hydrogen bonding interaction with Tyr170 and Asn108 residues; these two interactions are common to **10r** as well as to **5**. In addition, **10r** shows hydrogen bonding interaction with Ser111 and Leu46 residues.

These additional stabilizing interactions ensure that **10r** adopts a slightly different (and improved) pose in comparison to that of **5**. These improved interactions can be considered as deterministic factors for the improved anti-plasmodial activity of **10r**.

4. Conclusions

An efficacious transformation for converting readily available 3, 4-dihydropyrimidinones (DHPMs) to 2-aminopyrimidine based 4-aminoquinolines is presented. The compounds showed anti-plasmodial activity identical to or superior to CQ. Structure–activity relationship has been drawn leading to the identification of at least one compound **10r** as lead compound in this series. The tested compounds did not depict any antiviral activity and were cytotoxic. Binding interaction of representative potent compounds with heme and μ -oxo heme using UV–visible and NMR experiments furnished log *K* values identical with CQ binding and pointed to 1:1 stoichiometry of the most stable complexes in solution. DNA (both GC and AT rich) binding affinity using absorption and spectrofluorometric data indicated stronger interaction of **10c** (20 fold) than **10r** with CT DNA, however, **10r** showed higher affinity toward AT rich pUC18 DNA suggesting targeting of parasite AT rich DNA by **10r** in addition to β -hematin inhibition as possible mode of action of these compounds. DNA melting experiments suggested primary groove binding and/or partial intercalative nature of interaction of **10c** and **10r** with CT DNA. Thus, the strong electrostatic interaction of newly designed pyrimidine analogs with AT rich DNA and blockage of heme polymerisation by complexation of drug with heme contribute to the observed antimalarial activity in nano molar range. Further, molecular docking analysis of **10r** in the active site of *Pf* DHFR indicated superior binding compared to WR99210. Thus, drug **10r** acts on multiple targets (Heme, Enzyme involved in biosynthesis of DNA (DHFR), parasite DNA) which accounts for its high anti-plasmodial activity.

5. Experimental

5.1. General

All liquid reagents were dried/purified following recommended drying agents and/or distilled over 4 Å molecular sieves. THF was dried (Na- benzophenone ketyl) under nitrogen. ^1H NMR (300 MHz) and ^{13}C (75 MHz) NMR spectra were recorded in CDCl_3 on a multinuclear Jeol FT-AL-300 spectrometer with chemical shifts being reported in parts per million (δ) relative to internal tetramethylsilane (TMS, δ 0.0, ^1H NMR) or chloroform (CDCl_3 , δ 77.0, ^{13}C NMR). Mass spectra were recorded from Indian Institute of

Integrative Medicine (CSIR), Jammu, under electron impact at 70 eV on a Bruker Daltonics Esquire 3000 spectrometer. Elemental analysis was performed on FLASH EA 112 (Thermo electron Corporation) analyzer at Department of Chemistry, Guru Nanak Dev University, Amritsar and the results are quoted in %. IR recorded on FTIR Shimadzu 8400 Fourier-transform spectrophotometer in the range 400–4000 cm^{-1} using chloroform as medium. Melting points were determined in open capillaries and are uncorrected. For monitoring the progress of a reaction and for comparison purpose, thin layer chromatography (TLC) was performed on pre-coated aluminum sheets Merck (60F₂₅₄, 0.2 mm) using an appropriate solvent system. The chromatograms were visualized under UV light. For column chromatography silica gel (60–120 mesh) was employed and eluents were ethyl acetate/hexane or ethyl acetate/methanol mixtures.

5.2. General procedure for the synthesis of 2-aminopyrimidines (**10a–g** and **10j–s**)

To the stirred solution of **8** (2 mmol) and potassium carbonate (5 mmol) in dry THF (30 ml), a solution of appropriate 4-aminoquinoline **9** (1.0 mmol) in dry THF (50 ml) was added. The reaction mixture was stirred for 48 h at room temperature. The reaction mixture was filtered and THF was removed under vacuum. The residue was purified by column chromatography using MeOH/EtOAc as eluent to obtain corresponding **10**, which was recrystallized from DCM/hexane. Using this procedure the following compounds were isolated.

5.2.1. 5-Ethoxycarbonyl-6-methyl-4-phenyl-2-[(7-chloroquinolin-4-ylamino)ethylamino] pyrimidine (**10a**)

White solid. Rf: 0.4 (8% MeOH/EtOAc). Yield: 89%. IR (KBr): ν_{max} 770, 1267, 1709, 2928, 3331 cm^{-1} ^1H (300 MHz, CDCl_3 , 25 °C): δ 1.00 (t, $J = 7.2$ Hz, 3H, ester- CH_3), 2.55 (s, 3H, C6- CH_3), 3.47 (m, $J = 4.5$ Hz, 2H, CH_2), 3.94 (m, 2H, CH_2), 4.10 (q, $J = 7.2$ Hz, 2H, ester- CH_2), 5.81 (br, 1H, NH), 6.34 (d, 1H, ArH), 6.44 (br, 1H, NH), 7.26–7.85 (m, 8H, ArH), 8.44 (s, 1H, ArH). ^{13}C NMR (75 MHz, CDCl_3 , 25 °C): δ 13.5, 23.0, 40.1, 61.3, 98.4, 116.4, 121.3, 124.8, 128.1, 128.3, 128.6, 138.6, 148.8, 149.9, 151.8, 162.1 and 168.3. Anal. Calcd. for $\text{C}_{25}\text{H}_{24}\text{N}_5\text{O}_2\text{Cl}$: C, 65.00; H, 5.20; N, 15.10; Found: C, 64.92; H, 4.89; N, 15.32. MS: m/z 462 ($\text{M}^+ + 1$).

5.2.2. 5-Ethoxycarbonyl-6-methyl-4-phenyl-2-[(7-chloroquinolin-4-ylamino)propylamino]pyrimidine (**10b**)

White solid. Rf: 0.6 (8% MeOH/EtOAc). Yield: 84%. IR (KBr): ν_{max} 772, 1268, 1707, 2933, 3397 cm^{-1} ^1H (300 MHz, CDCl_3 , 25 °C): δ 0.95 (t, $J = 7.2$ Hz, 3H, ester- CH_3), 1.98 (q, $J = 6.3$ Hz, 2H, CH_2), 2.50 (s, 3H, C6- CH_3), 3.45 (q, $J = 6.3$ Hz, 2H, CH_2), 3.66 (q, $J = 6.6$ Hz, 2H, CH_2), 4.1 (q, $J = 7.2$ Hz, 2H, ester- CH_2), 5.63 (s, 1H, NH), 6.39 (d, $J = 5.4$ Hz, 1H, ArH), 7.38–7.54 (m, 7H, ArH), 7.90 (d, $J = 1.8$ Hz, 1H, ArH), 8.48 (d, $J = 5.4$ Hz, 1H, ArH). ^{13}C NMR (75 MHz, CDCl_3 , 25 °C): δ 13.5, 23.0, 38.2, 39.8, 61.1, 98.8, 117.2, 121.0, 125.1, 127.7, 128.4, 129.6, 134.7, 149.0, 149.6, 151.8, 161.6, 167.4 and 168.4. Anal. Calcd. For $\text{C}_{26}\text{H}_{26}\text{N}_5\text{O}_2\text{Cl}$: C, 65.60; H, 5.46; N, 14.70; Found: C, 65.59; H, 5.40; N, 14.50. MS: m/z 476.1 (M^+).

5.2.3. 5-Ethoxycarbonyl-6-methyl-4-phenyl-2-[(7-chloroquinolin-4-ylamino)butylamino]pyrimidine (**10c**)

White solid. Rf: 0.4 (EtOAc). Yield: 77%. IR (KBr): ν_{max} 772, 1268, 1708, 2986, 3383 cm^{-1} ^1H (300 MHz, CDCl_3 , 25 °C): δ 0.94 (t, $J = 7.2$ Hz, 3H, ester- CH_3), 1.80 (q, $J = 6.9$ Hz, 4H, CH_2), 2.47 (s, 3H, C6- CH_3), 3.37 (q, $J = 6.3$ Hz, 2H, CH_2), 3.60 (q, $J = 7.2$ Hz, 2H, CH_2), 4.05 (q, $J = 7.2$ Hz, 2H, ester- CH_2), 5.06 (s, 1H, NH), 5.45 (s, 1H, NH), 6.38 (d, $J = 5.4$ Hz, 1H, ArH), 7.3–7.58 (m, 7H, ArH), 7.94 (d, $J = 2.1$ Hz, 1H, ArH), 8.51 (d, $J = 5.4$ Hz, 1H, ArH). ^{13}C NMR (75 MHz, CDCl_3 , 25 °C):

δ 13.5, 22.9, 25.8, 27.4, 40.6, 42.9, 61.1, 99.0, 115.4, 117.0, 120.8, 125.2, 127.8, 128.2, 128.7, 129.4, 134.8, 139.0, 149.0, 149.6, 151.9, 161.2 and 168.7. Anal. Calcd. For $C_{27}H_{28}N_5O_2Cl$: C, 66.18; H, 5.72; N, 14.30; Found: C, 66.10; H, 5.63; N, 13.95. MS: m/z 490.1 (M^+).

5.2.4. 5-Ethoxycarbonyl-6-methyl-4-phenyl-2-[(7-chloroquinolin-4-ylamino)heptylamino]pyrimidine (**10d**)

White solid. Rf: 0.5 (EtOAc). Yield: 67%. IR (KBr): ν_{max} 769, 1264, 1700, 2930, 3278 cm^{-1} 1H (300 MHz, $CDCl_3$, 25 °C): δ 0.95 (t, $J = 7.2$ Hz, 3H, ester- CH_3), 1.44–2.00 (m, 10H, CH_2), 2.48 (s, 3H, C6- CH_3), 3.29 (d, $J = 5.1$ Hz, 2H, CH_2), 3.49 (t, $J = 6.3$ Hz, 2H, CH_2), 4.05 (q, $J = 7.2$ Hz, 2H, ester- CH_2), 4.93 (br, 1H, NH), 5.29 (br, 1H, NH), 6.40 (d, $J = 5.4$ Hz, 1H, ArH), 7.34–7.65 (m, 7H, ArH), 7.96 (d, $J = 1.8$ Hz, 1H, ArH), 8.53 (d, $J = 5.7$ Hz, 1H, ArH). ^{13}C NMR (75 MHz, $CDCl_3$, 25 °C): δ 13.0, 22.5, 26.2, 26.6, 28.4, 28.6, 29.0, 40.7, 42.8, 98.6, 116.6, 120.3, 123.5, 124.8, 127.5, 127.7, 128.4, 128.9, 134.4, 138.8, 148.7, 149.2, 151.6, 160.9 and 168.4. Anal. Calcd. For $C_{30}H_{34}N_5O_2Cl$: C, 67.13; H, 6.39; N, 13.17; Found: C, 67.43; H, 6.05; N, 13.45. MS: m/z 532.1 (M^+).

5.2.5. 5-Ethoxycarbonyl-6-methyl-4-phenyl-2-[(7-chloroquinolin-4-ylamino)octylamino]pyrimidine (**10e**)

White solid. Rf: 0.6 (EtOAc). Yield: 72%. IR (KBr): ν_{max} 770, 1263, 1712, 2928, 3269 cm^{-1} 1H (300 MHz, $CDCl_3$, 25 °C): δ 0.87 (t, $J = 7.6$ Hz, 3H, ester- CH_3), 1.30 (br, 10H, CH_2), 1.52 (d, $J = 6.6$ Hz, 2H, CH_2), 1.65 (q, $J = 6.9$ Hz, 2H, CH_2), 2.40 (s, 3H, C6- CH_3), 3.21 (d, $J = 7.2$ Hz, 2H, CH_2), 3.41 (t, $J = 6.6$ Hz, 2H, CH_2), 3.97 (q, $J = 7.2$ Hz, 2H, ester- CH_2), 5.13 (br, 1H, NH), 5.28 (br, 1H, NH), 6.31 (d, $J = 5.7$ Hz, 1H, ArH), 7.18–7.60 (m, 7H, ArH), 7.86 (d, $J = 1.8$ Hz, 1H, ArH), 8.42 (d, $J = 5.1$ Hz, 1H, ArH). ^{13}C NMR (75 MHz, $CDCl_3$, 25 °C): δ 13.5, 22.9, 26.7, 27.0, 28.8, 29.1, 29.2, 29.5, 41.2, 43.2, 61.0, 99.0, 115.1, 117.0, 120.8, 125.2, 127.9, 128.2, 128.8, 129.3, 134.8, 139.2, 149.0, 149.7, 152.0, 161.2 and 168.9. Anal. Calcd. For $C_{31}H_{36}N_5O_2Cl$: C, 68.19; H, 6.59; N, 12.8; Found: C, 68.03; H, 6.55; N, 12.02. MS: m/z 546.2 (M^+).

5.2.6. 5-Ethoxycarbonyl-6-methyl-4-phenyl-2-[(7-chloroquinolin-4-ylamino)decylamino]pyrimidine (**10f**)

Viscous liquid. Rf: 0.3 (1% MeOH/EtOAc). Yield: 64%. IR (KBr): ν_{max} 775, 1256, 1708, 2985, 3325 cm^{-1} 1H (300 MHz, $CDCl_3$, 25 °C): δ 0.86 (t, $J = 7.2$ Hz, 3H, ester- CH_3), 1.25 (br, 14H, CH_2), 1.52 (q, $J = 6.9$ Hz, 2H, CH_2), 1.67 (q, $J = 6.6$ Hz, 2H, CH_2), 2.41 (s, 3H, C6- CH_3), 3.22 (q, $J = 7.2$ Hz, 2H, CH_2), 3.41 (t, $J = 6.6$ Hz, 2H, CH_2), 3.97 (q, $J = 6.9$ Hz, 2H, ester- CH_2), 5.04 (br, 1H, NH), 5.30 (br, 1H, NH), 6.32 (d, $J = 5.4$ Hz, 1H, ArH), 7.19–7.61 (m, 7H, ArH), 7.88 (d, $J = 2.1$ Hz, 1H, ArH), 8.44 (d, $J = 5.7$ Hz, 1H, ArH). ^{13}C NMR (75 MHz, $CDCl_3$, 25 °C): δ 13.5, 14.5, 26.8, 27.1, 28.8, 29.2, 29.3, 29.4, 29.6, 41.3, 43.3, 61.0, 99.0, 115.0, 117.0, 120.8, 125.3, 127.9, 128.2, 128.5, 129.4, 134.9, 139.2, 149.8, 151.6, 161.2. Anal. Calcd. For $C_{33}H_{40}N_5O_2Cl$: C, 69.00; H, 6.97; N, 12.20; Found: C, 68.93; H, 6.66; N, 11.82. MS: m/z 574.2 (M^+).

5.2.7. 5-Ethoxycarbonyl-6-methyl-4-phenyl-2-[(7-chloroquinolin-4-ylamino)dodecylamino]pyrimidine (**10g**)

Viscous liquid. Rf: 0.4 (1% MeOH/EtOAc). Yield: 65%. IR (KBr): ν_{max} 772, 1270, 1700, 2998, 3300 cm^{-1} 1H (300 MHz, $CDCl_3$, 25 °C): δ 0.93 (t, $J = 7.2$ Hz, 3H, ester- CH_3), 1.26 (s, 16H, CH_2), 1.57 (d, $J = 6.9$ Hz, 2H, CH_2), 1.71 (d, $J = 6.9$ Hz, 2H, CH_2), 2.48 (s, 3H, C6- CH_3), 3.24 (s, 2H, CH_2), 3.45 (q, $J = 6.6$ Hz, 2H, CH_2), 4.04 (q, $J = 7.2$ Hz, 2H, ester- CH_2), 5.71 (br, 1H, NH), 6.18 (d, $J = 5.4$ Hz, 1H, ArH), 6.74 (br, 1H, NH), 7.23–7.40 (m, 7H, ArH), 7.83 (d, $J = 6.9$ Hz, 1H, ArH), 8.23 (s, 1H, ArH). ^{13}C NMR (75 MHz, $CDCl_3$, 25 °C): δ 13.5, 22.9, 26.8, 27.1, 28.9, 29.2, 29.3, 29.4, 29.5, 41.3, 43.3, 60.9, 99.0, 115.0, 117.0, 120.7, 125.2, 127.9, 128.1, 128.7, 129.3, 134.8, 139.2, 148.9, 149.7, 151.9, 161.2 and 168.9. Anal. Calcd. For $C_{35}H_{44}N_5O_2Cl$: C, 69.82; H, 7.30; N, 11.63; Found: C, 69.53; H, 6.96; N, 11.45. MS: m/z 602 (M^+).

5.2.8. 5-Ethoxycarbonyl-6-methyl-4-phenyl-2-[(7-chloroquinolin-4-ylamino)propylamino]pyrimidine (**10j**)

White solid. Rf: 0.7 (5% MeOH/EtOAc). Yield: 58%. IR (KBr): ν_{max} 716, 1127, 1700, 2940, 3446 cm^{-1} 1H (300 MHz, $CDCl_3$, 25 °C): δ 1.00 (t, $J = 7.2$ Hz, 3H, ester- CH_3), 1.46 (d, $J = 6.6$ Hz, 3H, CH_3), 2.54 (s, 3H, C6- CH_3), 4.10 (q, $J = 6.0$ Hz, 2H, ester- CH_2), 4.69 (m, 1H, CH), 5.35 (br, 1H, NH), 6.39 (d, $J = 5.4$ Hz, 1H, ArH), 6.60 (br, 1H, NH), 7.50–7.84 (m, 8H, ArH), 8.42 (s, 1H, ArH). ^{13}C NMR (75 MHz, $CDCl_3$, 25 °C): δ 13.1, 19.1, 22.5, 29.2, 45.9, 60.9, 98.1, 120.9, 124.4, 127.7, 127.8, 128.0, 128.1, 128.2, 128.3, 138.2, 149.5, 151.5, 161.1 and 167.9. Anal. Calcd. For $C_{26}H_{26}N_5O_2Cl$: C, 65.60; H, 5.46; N, 14.70; Found: C, 65.39; H, 5.43; N, 14.45. MS: m/z 475.5 (M^+).

5.2.9. 5-Ethoxycarbonyl-6-methyl-4-phenyl-2-[5-(7-chloroquinolin-4-ylamino)-2-methylpentylamino]pyrimidine (**10k**)

Viscous liquid. Rf: 0.6 (8% MeOH/EtOAc). Yield: 55%. IR (KBr): ν_{max} 716, 1127, 1700, 2940, 3446 cm^{-1} 1H (300 MHz, $CDCl_3$, 25 °C): δ 1.03–1.16 (m, 7H, ester- CH_3 & $2 \times CH_2$), 1.36 (d, $J = 1.5$ Hz, 3H, CH_3), 2.58 (s, 3H, C6- CH_3), 3.64 (m, 4H, $2 \times CH_2$), 4.12–4.24 (m, 3H, CH & ester- CH_2), 5.24 (br, 1H, NH), 5.64 (br, 1H, NH), 6.48 (s, $J = 5.4$ Hz, 1H, ArH), 7.37–7.72 (m, 8H, ArH), 8.07 (s, 1H, ArH), 8.60 (s, 1H, ArH). ^{13}C NMR (75 MHz, $CDCl_3$, 25 °C): δ 13.4, 17.8, 17.9, 26.1, 26.9, 31.5, 31.7, 32.3, 33.1, 41.3, 43.4, 46.8, 49.3, 61.0, 98.9, 115.3, 120.8, 120.9, 125.3, 127.8, 128.1, 128.3, 128.4, 129.4, 135.0, 139.0, 150.0, 151.5 and 168.7. Anal. Calcd. For $C_{29}H_{32}N_5O_2Cl$: C, 67.23; H, 6.23; N, 13.52; Found: C, 67.09; H, 6.12; N, 13.36. MS: m/z 518 (M^+).

5.2.10. 5-Ethoxycarbonyl-6-methyl-4-methyl-2-[(7-chloroquinolin-4-ylamino)propylamino]pyrimidine (**10l**)

White solid. Rf: 0.5 (10% MeOH/EtOAc). Yield: 92%. IR (KBr): ν_{max} 801, 1261, 1701, 2930, 3419 cm^{-1} 1H (300 MHz, $CDCl_3$, 25 °C): δ 1.38 (t, $J = 7.2$ Hz, 3H, ester- CH_3), 2.01 (m, 2H, CH_2), 2.44 (s, 6H, C6 & C4- CH_3), 3.44 (q, $J = 6.0$ Hz, 2H, CH_2), 3.67 (q, $J = 6.3$ Hz, 2H, CH_2), 4.36 (q, $J = 7.2$ Hz, 2H, ester- CH_2), 5.57 (br, 1H, NH), 5.64 (br, 1H, NH), 6.42 (d, $J = 5.4$ Hz, 1H, ArH), 7.33 (m, 1H, ArH), 7.73 (d, $J = 9.0$ Hz, 1H, ArH), 7.96 (d, $J = 2.1$ Hz, 1H, ArH), 8.52 (d, $J = 5.4$ Hz, 1H, ArH). ^{13}C NMR (75 MHz, $CDCl_3$, 25 °C): δ 14.2, 23.7, 29.0, 38.3, 40.0, 61.0, 99.0, 121.1, 125.2, 128.8, 134.9, 149.7, 151.9, 161.3 and 167.3. Anal. Calcd. For $C_{21}H_{24}N_5O_2Cl$: C, 58.04; H, 5.80; N, 16.90; Found: C, 57.84; H, 5.93; N, 16.63. MS: m/z 413.5 (M^+).

5.2.11. 5-Ethoxycarbonyl-6-methyl-4-methyl-2-[(7-chloroquinolin-4-ylamino)butylamino]pyrimidine (**10m**)

White solid. Rf: 0.6 (10% MeOH/EtOAc). Yield: 90%. IR (KBr): ν_{max} 760, 1257, 1695, 2935, 3431 cm^{-1} 1H (300 MHz, $CDCl_3$, 25 °C): δ 1.37 (t, $J = 6.9$ Hz, 3H, ester- CH_3), 1.82 (m, 4H, CH_2), 2.41 (s, 6H, C6 & C4- CH_3), 3.40 (q, $J = 6.9$ Hz, 2H, CH_2), 3.57 (q, $J = 6.0$ Hz, 2H, CH_2), 4.35 (q, $J = 7.2$ Hz, 2H, ester- CH_2), 5.10 (br, 1H, NH), 5.23 (br, 1H, NH), 6.42 (d, $J = 5.4$ Hz, 1H, ArH), 7.34 (m, 1H, ArH), 7.64 (d, $J = 9.0$ Hz, 1H, ArH), 7.96 (d, $J = 2.1$ Hz, 1H, ArH), 8.53 (d, $J = 5.1$ Hz, 1H, ArH). ^{13}C NMR (75 MHz, $CDCl_3$, 25 °C): δ 9.8, 12.0, 13.6, 26.8, 29.1, 47.1, 85.2, 106.9, 111.5, 114.9 and 138.0. Anal. Calcd. For $C_{22}H_{26}N_5O_2Cl$: C, 61.75; H, 6.08; N, 16.37; Found: C, 61.43; H, 6.15; N, 15.99. MS: m/z 428.1 (M^+).

5.2.12. 5-Isopropoxyloxycarbonyl-6-methyl-4-(3-nitrophenyl)-2-[(7-chloroquinolin-4-ylamino)propyl amino]pyrimidine (**10n**)

Yellow solid. Rf: 0.6 (2% MeOH/EtOAc). Yield: 71%. IR (KBr): ν_{max} 752, 1356, 1527, 1700, 2973, 3421 cm^{-1} 1H (300 MHz, $CDCl_3$, 25 °C): δ 1.09 (d, $J = 6.0$ Hz, 6H, $2 \times$ ester- CH_3), 2.09 (m, 2H, CH_2), 2.52 (s, 3H, C6- CH_3), 3.46 (q, $J = 6.0$ Hz, 2H, CH_2), 3.71 (q, $J = 6.6$ Hz, 2H, CH_2), 5.06 (m, 1H, ester-CH), 5.40 (br, 1H, NH), 5.59 (br, 1H, NH), 6.40 (d, $J = 5.4$ Hz, 1H, ArH), 7.23–7.28 (m, 2H, ArH), 7.55 (t, $J = 7.8$ Hz, 1H, ArH), 7.81 (d, $J = 3.3$ Hz, 1H, ArH), 7.94 (d, $J = 2.1$ Hz, 1H, ArH), 8.26 (d, $J = 1.5$ Hz, 1H, ArH), 8.42 (t, $J = 2.1$ Hz, 1H, ArH), 8.50 (d, $J = 5.4$ Hz, 1H,

ArH). ^{13}C NMR (75 MHz, CDCl_3 , 25°C): δ 21.3, 21.4, 28.9, 38.7, 40.3, 69.4, 99.0, 120.8, 123.2, 124.1, 125.1, 128.7, 129.3, 133.9, 149.5 and 161.4. Anal. Calcd. For $\text{C}_{27}\text{H}_{27}\text{N}_6\text{O}_4\text{Cl}$: C, 60.60; H, 5.05; N, 15.70; Found: C, 60.23; H, 5.02; N, 15.49. MS: m/z 534.5 (M^+).

5.2.13. 5-Isopropoxyloxycarbonyl-6-methyl-4-(3-nitrophenyl)-2-[(7-chloroquinolin-4-ylamino)butylamino] pyrimidine (**10o**)

Yellow solid. Rf: 0.6 (5% MeOH/EtOAc). Yield: 78%. IR (KBr): ν_{max} 760, 1357, 1526, 1710, 2935, 3412 cm^{-1} ^1H (300 MHz, CDCl_3 , 25°C): δ 1.2 (d, $J = 6.0$ Hz, 6H, $2 \times$ ester- CH_3), 1.84 (m, 4H, CH_2), 2.55 (s, 3H, C_6-CH_3), 3.37 (m, 2H, CH_2), 3.58 (m, 2H, CH_2), 5.03 (m, 1H, ester-CH), 5.41 (br, 1H, NH), 5.60 (br, 1H, NH), 6.33 (d, $J = 5.4$ Hz, 1H, ArH), 7.27–7.30 (m, 2H, ArH), 7.81 (t, $J = 1.2$ Hz, 1H, ArH), 7.83 (d, $J = 1.2$ Hz, 1H, ArH), 7.84 (s, 1H, ArH), 7.92 (d, $J = 2.1$ Hz, 1H, ArH), 8.43 (d, $J = 5.7$ Hz, 2H, ArH). ^{13}C NMR (75 MHz, CDCl_3 , 25°C): δ 21.2, 25.7, 28.1, 42.8, 69.2, 98.7, 115.5, 116.7, 121.2, 123.2, 123.9, 125.2, 127.6, 129.0, 133.9, 135.1, 140.5, 147.9, 150.1, 150.7, 161.0 and 167.3. Anal. Calcd. For $\text{C}_{28}\text{H}_{29}\text{N}_6\text{O}_4\text{Cl}$: C, 61.20; H, 5.28; N, 15.30; Found: C, 60.58; H, 5.48; N, 15.18. MS: m/z 548.1 (M^+).

5.2.14. 5-Isopropoxyloxycarbonyl-6-methyl-4-(2-nitrophenyl)-2-[(7-chloroquinolin-4-ylamino)ethylamino] pyrimidine (**10p**)

Yellow solid. Rf: 0.5 (5% MeOH/EtOAc). Yield: 66%. IR (KBr): ν_{max} 760, 1353, 1528, 1709, 2975, 3364 cm^{-1} ^1H (300 MHz, CDCl_3 , 25°C): δ 0.93 (d, $J = 6.3$ Hz, 6H, $2 \times$ ester- CH_3), 2.67 (s, 3H, C_6-CH_3), 3.53 (br, 2H, CH_2), 3.85 (br, 2H, CH_2), 4.98 (m, 1H, ester-CH), 5.74 (br, 1H, NH), 6.45 (d, $J = 5.1$ Hz, 1H, ArH), 7.20–7.60 (m, 6H, ArH), 7.68 (s, 1H, ArH), 8.17 (d, $J = 8.1$ Hz, 1H, ArH), 8.44 (s, 1H, ArH). ^{13}C NMR (75 MHz, CDCl_3 , 25°C): δ 21.2, 40.13, 68.7, 98.9, 124.4, 125.1, 128.7, 129.4, 129.8, 134.7 and 151.9. Anal. Calcd. For $\text{C}_{26}\text{H}_{27}\text{N}_6\text{O}_4\text{Cl}$: C, 59.90; H, 4.80; N, 16.10; Found: C, 60.04; H, 4.69; N, 15.88. MS: m/z 520.1 (M^+).

5.2.15. 5-Isopropoxyloxycarbonyl-6-methyl-4-(2-nitrophenyl)-2-[(7-chloroquinolin-4-ylamino)propyl amino] pyrimidine (**10q**)

Yellow solid. Rf: 0.6 (10% MeOH/EtOAc). Yield: 85%. IR (KBr): ν_{max} 757, 1346, 1529, 1705, 2973, 3351 cm^{-1} (300 MHz, CDCl_3 , 25°C): δ 0.90 (s, 6H, $2 \times$ ester- CH_3), 2.04 (m, 2H, CH_2), 2.57 (s, 3H, C_6-CH_3), 3.19 (br, 2H, CH_2), 3.41 (q, $J = 5.4$ Hz, 2H, CH_2), 3.57 (br, 1H, NH), 4.87 (m, 1H, ester-CH), 6.03 (br, 1H, NH), 6.34 (d, $J = 5.7$ Hz, 1H, ArH), 7.27–7.64 (m, 5H, ArH), 7.90 (s, 1H, ArH), 8.11 (d, $J = 7.8$ Hz, 1H, ArH), 8.42 (t, $J = 5.4$ Hz, 1H, ArH). ^{13}C NMR (75 MHz, CDCl_3 , 25°C): δ 21.1, 24.1, 28.5, 38.2, 39.9, 68.5, 98.5, 114.3, 116.8, 121.5, 124.3, 125.4, 126.5, 129.4, 129.7, 133.1, 135.5, 135.6, 149.7, 150.7, 161.0 and 165.6. Anal. Calcd. For $\text{C}_{27}\text{H}_{27}\text{N}_6\text{O}_4\text{Cl}$: C, 60.60; H, 5.05; N, 15.70; Found: C, 60.39; H, 4.82; N, 15.88. MS: m/z 534.5 (M^+).

5.2.16. 5-Isopropoxyloxycarbonyl-6-methyl-4-(2-nitrophenyl)-2-[(7-chloroquinolin-4-ylamino)butylamino] pyrimidine (**10r**)

Yellow solid. Rf: 0.6 (5% MeOH/EtOAc). Yield: 85%. IR (KBr): ν_{max} 785, 1266, 1346, 1526, 1713, 2932, 3415 cm^{-1} ^1H (300 MHz, CDCl_3 , 25°C): δ 0.89 (d, $J = 6.3$ Hz, 6H, $2 \times$ ester- CH_3), 1.76 (m, 4H, CH_2), 2.57 (s, 3H, C_6-CH_3), 3.13 (br, 1H, NH), 3.30 (m, 2H, CH_2), 3.53 (m, 2H, CH_2), 4.87 (m, 1H, ester-CH), 5.50 (br, 1H, NH), 6.34 (s, 1H, ArH), 7.25–7.58 (m, 4H, ArH), 7.70 (d, $J = 8.4$ Hz, 1H, ArH), 7.94 (d, $J = 1.5$ Hz, 1H, ArH), 8.49 (d, $J = 5.4$ Hz, 1H, ArH). ^{13}C NMR (75 MHz, CDCl_3 , 25°C): δ 20.8, 20.9, 21.1, 25.6, 29.6, 41.0, 42.8, 42.9, 69.9, 70.1, 98.8, 116.9, 121.5, 124.3, 124.6, 125.3, 127.7, 129.5, 129.7, 130.1, 130.2, 133.3, 135.1, 150.1, 150.2, 150.8, 151.0 and 160.1. Anal. Calcd. For $\text{C}_{28}\text{H}_{29}\text{N}_6\text{O}_4\text{Cl}$: C, 61.20; H, 5.28; N, 15.30; Found: C, 60.97; H, 4.93; N, 15.25. MS: m/z 548.1 (M^+).

5.2.17. 5-Isopropoxyloxycarbonyl-6-methyl-4-(4-nitrophenyl)-2-[(7-chloroquinolin-4-ylamino)propyl amino] pyrimidine (**10s**)

Yellow solid. Rf: 0.9 (1% MeOH/EtOAc). Yield: 82%. IR (KBr): ν_{max} 761, 1271, 1346, 1527, 1710, 2938, 3400 cm^{-1} ^1H (300 MHz, CDCl_3 ,

25°C): δ 1.05 (s, 6H, $2 \times$ ester- CH_3), 2.05 (q, $J = 4.2$ Hz, 2H, CH_2), 2.51 (s, 3H, C_6-CH_3), 3.46 (t, $J = 6$ Hz, 2H, CH_2), 3.70 (d, $J = 6.3$ Hz, 2H, CH_2), 4.98 (m, 1H, ester-CH), 6.39 (d, $J = 5.1$ Hz, 1H, ArH), 7.63 (d, $J = 6.0$ Hz, 4H, ArH), 7.90–8.40 (m, 3H, ArH), 8.49 (d, $J = 5.1$ Hz, 1H, ArH). ^{13}C NMR (75 MHz, CDCl_3 , 25°C): δ 13.4, 13.5, 20.5, 29.4, 29.7, 31.5, 55.0, 61.6, 61.7, 72.3, 111.5, 126.5, 126.6, 128.0, 128.3, 128.4, 128.9, 129.0, 130.9, 142.6, 158.2 and 166.1. Anal. Calcd. For $\text{C}_{27}\text{H}_{27}\text{N}_6\text{O}_4\text{Cl}$: C, 60.60; H, 5.05; N, 15.70; Found: C, 60.23; H, 4.97; N, 15.45. MS: m/z 534.5 (M^+).

5.3. General procedure for the synthesis of 2-aminopyrimidines (**10h & 10i**)

To the stirred solution of appropriate 4-aminoquinoline **9** in dry THF (50 ml) mixture of **8** (in a 1:2 molar ratio) and potassium carbonate in dry acetonitrile was added. The reaction mixture was refluxed for 48 h and then filtered. Acetonitrile was removed under vacuum and the residue was purified by column chromatography using EtOAc/hexane as eluent to give **10h** and **10i** which were recrystallized from DCM/hexane.

5.3.1. 5-Ethoxycarbonyl-6-methyl-4-phenyl-2-[2-(7-chloroquinolin-4-ylamino)phenylamino] pyrimidine (**10h**)

Yellow solid. Rf: 0.9 (70% Hexane/EtOAc). Yield: 53%. IR (KBr): ν_{max} 770, 1253, 1717, 2923, 2970, 3192, 3389 cm^{-1} ^1H (300 MHz, CDCl_3 , 25°C): δ 0.99 (t, $J = 7.2$ Hz, 3H, ester- CH_3), 2.51 (s, 3H, C_6-CH_3), 3.81 (br, 1H, NH), 4.09 (q, $J = 7.2$ Hz, 2H, ester- CH_2), 4.13 (br, 1H, NH), 6.81–6.91 (m, 4H, ArH), 7.04 (t, 1H, ArH), 7.42 (t, $J = 1.8$ Hz, 4H, ArH), 7.51–7.59 (m, 5H, ArH). ^{13}C NMR (75 MHz, CDCl_3 , 25°C): δ 11.5, 20.9, 59.3, 115.4, 117.5, 122.8, 124.1, 126.0, 126.3 and 127.7. Anal. Calcd. For $\text{C}_{29}\text{H}_{24}\text{N}_5\text{O}_2\text{Cl}$: C, 68.30; H, 4.71; N, 13.70; Found: C, 68.15; H, 4.47; N, 13.57. MS: m/z 510.5 (M^+).

5.3.2. 5-Ethoxycarbonyl-6-methyl-4-phenyl-2-[4-(7-chloroquinolin-4-ylamino)phenylamino] pyrimidine (**10i**)

Yellow solid. Rf: 0.4 (50% Hexane/EtOAc). Yield: 57%. IR (KBr): ν_{max} 768, 1257, 1714, 2929, 3063, 3385 cm^{-1} ^1H (300 MHz, CDCl_3 , 25°C): δ 1.00 (t, $J = 7.2$ Hz, 3H, ester- CH_3), 2.58 (s, 3H, C_6-CH_3), 4.11 (q, $J = 7.2$ Hz, 2H, ester- CH_2), 6.60 (br, 1H, NH), 6.84 (d, $J = 5.4$ Hz, 1H, ArH), 7.22–7.87 (m, 11H, ArH), 8.02 (d, $J = 1.8$ Hz, 1H, ArH), 8.52 (d, $J = 2.7$ Hz, 1H, ArH). ^{13}C NMR (75 MHz, CDCl_3 , 25°C): δ 13.5, 29.6, 61.3, 76.5, 101.9, 117.5, 117.7, 120.3, 120.4, 121.1, 124.5, 125.9, 128.0, 128.4, 128.5, 128.9, 129.8, 133.8, 135.2, 136.7, 138.5, 148.3, 149.5, 151.8, 158.6, 165.9, 167.3 and 168.4. Anal. Calcd. For $\text{C}_{29}\text{H}_{24}\text{N}_5\text{O}_2\text{Cl}$: C, 68.30; H, 4.71; N, 13.70; Found: C, 67.99; H, 4.92; N, 13.57. MS: m/z 510.5 (M^+).

6. Materials and methods

6.1. In vitro anti-plasmodial activity assay

Two clones of *P. falciparum* are used: (a) 3D7 clone of NF54 which is known to be sensitive to all anti-plasmodials, (b) K1 strain originating from Thailand that is resistant to chloroquine and pyrimethamine, but sensitive to mefloquine. The cultures were naturally asynchronous (65–75% ring stage) and were maintained in continuous log phase growth in RPMI1640 medium supplemented with 5% washed human A+ erythrocytes, 25 mM Hepes, 32 nM NaHCO_3 , and AlbuMAXII (lipid-rich bovine serum albumin) (GIBCO, Grand Island, NY) (CM). All cultures and assays are conducted at 37°C under an atmosphere of 5% CO_2 and 5% O_2 with a balance of N_2 . Stock drug solutions were prepared in 100% DMSO (dimethylsulfoxide) at 20 mg/ml. The compound was further diluted to the appropriate concentration using complete medium RPMI1640 supplemented with 15 nM cold hypoxanthine and

AlbuMAXII. Assays were performed in sterile 96-well microtitre plates; each plate contained 100 μ l of parasite culture (0.5% parasitemia, 2.5% hematocrit). Each compound was tested in triplicate and parasite growth compared to control and blank (uninfected erythrocytes) wells. After 24 h of incubation at 37 °C, 3.7 Bq of [³H] hypoxanthine is added to each well [51]. Cultures were incubated for a further 24 h before they are harvested onto glass-fiber filter mats. The radioactivity was counted using a Wallac Microbeta 1450 scintillation counter. The results were recorded as counts per minute (CPM) per well at each drug concentration, control and blank wells. Percentage inhibition was calculated from comparison to blank and control wells, and IC₅₀ values calculated using Graph Pad Prism 4.0. The preliminary screen uses the 3D7 strain. The compounds were tested at 6 concentrations (30, 10, 3, 1, 0.3, and 0.1 μ g/ml). If the compound did not affect parasite growth at 10 μ g/ml it was classified as inactive, between 10 and 1 μ g/ml, the compound was designated as partially active, and if <1 μ g/ml, the compound was classified as active and was further evaluated by three-fold serial dilutions in a repeat test. For secondary screening both the 3D7 clone and the K1 line were used. The compound was diluted three-fold over at 12 different concentrations with an appropriate starting concentration based on the preliminary screen. The IC₅₀ is determined by a sigmoidal dose response analysis using Graph Pad Prism 4.0. For each assay, the IC₅₀ and IC₉₀ values for each parasite line were determined against the known anti-plasmodials chloroquine and artesunate.

6.2. Cytotoxicity and antiviral assay

The antiviral assays [except anti-human immunodeficiency virus (HIV) assays] were based on inhibition of virus-induced cytopathicity in HEL [herpes simplex virus type 1 (HSV-1), HSV-2 (G), vaccinia virus, and vesicular stomatitis virus], Vero (para-influenza-3, reovirus-1, Coxsackie B4, and Punta Toro virus), HeLa (vesicular stomatitis virus, Coxsackie virus B4, and respiratory syncytial virus) and MDCK (influenza A (H1N1; H3N2) and B virus) cell cultures. Confluent cell cultures in microtiter 96-well plates were inoculated with 100 cell culture inhibitory dose-50 (CCID₅₀) of virus (1 CCID₅₀ being the virus dose to infect 50% of the cell cultures) in the presence of varying concentrations of the test compounds. Viral cytopathicity was recorded as soon as it reached completion in the control virus-infected cell cultures that were not treated with the test compounds. The anti-HIV activity and anti-proliferative activity were evaluated against HIV-1 strain IIIB and HIV-2 strain ROD in human T-lymphocyte CEM cell cultures. Briefly, virus stocks were titrated in CEM cells and expressed as the 50% cell culture infective dose (CCID₅₀). CEM cells were suspended in culture medium at $\sim 3 \times 10^5$ cells/ml and infected with HIV at ~ 100 CCID₅₀. Immediately after viral exposure, 100 μ l of the cell suspension was placed in each well of a flat-bottomed microtiter plate containing various concentrations of the test compounds. After a 4-day incubation period at 37 °C, the giant cell formation was microscopically determined. Compounds were tested in parallel for cytostatic activity in uninfected CEM cells.

6.3. Heme binding studies

6.3.1. Binding of **10c** & **10r** with monomeric heme

Hemin stock solution (1.2 mM) was prepared by dissolving (7.8 mg) hemin chloride in 10 ml AR grade DMSO. Working solutions (2.4 μ M) were prepared by mixing 20 μ l hemin stock solution with 4 ml DMSO and 1 ml 0.2 M HEPES buffer (pH 7.4) and making it up to 10 ml with double distilled deionized water. Stock solutions of **10c** and **10r** (2 mM) were prepared in AR grade DMSO and were used for titration experiment. Heme (2.4 μ M) was titrated with

increasing concentrations (0–70 μ M) of **10c** and **10r**. Following each addition, absorbance was recorded at 402 nm. For conducting the experiment at pH 5.6, solutions of **10c** and **10r** and Fe (III) PPIX were prepared in exactly the same manner, except that 2-[N-morpholino]ethanesulphonate (MES) buffer (pH 5.4) was substituted for HEPES buffer [31].

6.3.2. Binding of **10c** & **10r** with μ -oxo dimeric heme

Stock solution (10 mM) of heme was prepared by dissolving hemin chloride in 0.1 M NaOH. Solution was sonicated for 30 min to ensure complete dissolution. Heme stock solution was diluted to 60 μ M in phosphate buffer (20 mM, pH 5.8). Stock solution of **10c** and **10r** (2 mM) were prepared in AR grade DMSO. Titrations were performed by successive addition of aliquots of stock solution of **10c** or **10r** (0–15 μ L) to 60 μ M heme solution & changes in the absorbance at 362 nm were recorded. The association constants for both monomeric & μ -oxo dimeric heme were determined by using Hyp Spec [37].

6.3.3. Binding stoichiometry

Binding Stoichiometries of drug with monomeric & μ -oxo dimeric heme were monitored by UV–visible spectrophotometry using Job's method of continuous variation [33,34]. The concentration of drug & heme in solution was kept constant and changes in absorbance at 402 nm (monomeric)/362 nm (dimeric) were monitored as a function of the mole fraction.

6.3.4. Ferriprotoporphyrin IX biomineralisation inhibition test (FBIT)

96 well plate containing mixture of 50 μ l of 0.5 mg/ml of hemin chloride dissolved in DMSO, 100 μ l of 0.5 M sodium acetate buffer (pH 4.4) and 50 μ l of different concentrations of drug solution or 50 μ l of solvent (control), was incubated at 37 °C for 24 h. The plate was centrifuged at 4500 rpm for 3 min, and supernatant was discarded. The remaining pellet was re-suspended with 200 μ l of DMSO to eliminate unreacted hemin [38,39]. The plate was centrifuged again and supernatant similarly discarded. The precipitate was dissolved in 150 μ l of 0.1 N NaOH & absorbance was read at 405 nm. The percentage of inhibition of Ferriprotoporphyrin IX Biomineralisation was calculated using formula:

$$\text{Inhibition(\%)} = 100 \times \frac{[(\text{Abs of control}) - (\text{Abs of drug})]}{(\text{Abs of control})}$$

IC₅₀ values were determined by using Graph pad Prism 4.0.

6.4. DNA binding studies with **10c** and **10r**

6.4.1. Preparation of stock solutions

Stock solution of **10c** and **10r** (2 mM) were prepared in AR grade methanol. The DNA binding experiments were carried out by making dilution of the stock with 1:1 buffered methanol.

6.4.2. Preparation of CT DNA solution

Stock solution of DNA was prepared by dissolving DNA pellet in TE buffer (10 mM Tris–HCl, 0.1 mM EDTA, pH 7.4). The DNA concentration was estimated from its absorbance intensity at 260 nm with a known molar absorption coefficient value of 6600 dm³mol⁻¹cm⁻¹. The purity of DNA was established from ratio of absorbance intensity at 260 nm and at 280 nm. The observed ratio of 1.8 ensured that DNA was free from protein.

6.4.3. Evaluation of binding constant

6.4.3.1. UV-spectrophotometry. The titration experiment was performed by varying the concentration of CT DNA and keeping the drug concentration constant (30 μ M). All the UV–visible spectra were recorded after equilibration of solution for 5 min. The binding

constants were calculated from absorption at 331 nm by using Benesi–Hildebrand equation [48].

6.4.3.2. Spectrofluorometric titrations. The steady state fluorescence experiments were carried out on Varian Cary Eclipse Spectrofluorometer at ambient temperature. A slit width of 5 nm was used with $\lambda_{\text{ex}} = 320$ nm and $\lambda_{\text{em}} = 380$ nm. The titration experiment was accomplished by varying the concentration of DNA in cuvette (0.3–70 μM) and keeping the compound concentration constant (30 μM). In fluorescence titration experiment working solutions were prepared by making dilution of DNA stock and drug stock with methanol.

6.4.3.3. DNA thermal denaturation. DNA melting experiment were carried out by monitoring the absorbance of CT DNA (151 μM NP) at 260 nm at various temperature in the presence and absence of drug in a 5:1 ratio of the DNA and drug with a ramp rate of 0.5° C/min in a 40% DMSO/TE buffer (pH 7.4) with 0.5 mM NaCl on a Shimadzu 1601 PC spectrophotometer equipped with a Peltier thermo regulator. The thermal melting temperature was calculated by plotting dA/dT vs temperature using Microsoft Excel.

6.4.4. Molecular docking method

The molecular docking analysis was carried out using FlexX molecular docking module [52,53] (FlexX 1.13.5) available in the SYBYL 7.1 software package from Tripose [54]. This docking approach adopts an incremental construction algorithm for identifying appropriate pose of the substrate in the active site of the enzyme. It generates about 30 possible poses of the substrate in the active site. Most of the 30 poses obtained in this analysis adopted similar binding mode in the enzyme cavity and hence the top scoring pose was considered in this analysis. To perform the above analysis, the crystal structure 1J3I (Wild-type *Plasmodium falciparum* dihydrofolate reductase-thymidylate synthase (PfDHFR-TS) complexed with WR99210, NADPH, and dUMP) was downloaded from the protein data bank [55] (PDB) and subjected to protein preparation and receptor description [56]. The structures of the substrates were prepared by first building the molecules in 3D and optimizing the structures using tripos force field. The ionic, tautomeric states of substrates were considered while performing molecular docking analysis. The pose shown in Fig. 7 includes the neutral state of the substrate in the active site of the enzyme.

Acknowledgments

We thank CSIR [01/(2364)/10/EMR-II], UGC [F. No. 37-188/2009(SR)] and SAP (DRS-1) UGC, New Delhi and the KU Leuven (GOA no. 10/14) for providing financial support.

Appendix A. Supplementary data

Supplementary data related to this article can be found online at doi:10.1016/j.ejmech.2012.03.007.

References

- [1] T.N.C. Wells, P.L. Alonso, W.E. Gutteridge, New medicines to improve control and contribute to the eradication of malaria, *Nature* 8 (2009) 879–891.
- [2] R.E. Martin, R.V. Marchetti, A.I. Cowan, S.M. Howitt, S. Broer, K. Kirk, Chloroquine transport via the malaria parasite's chloroquine resistance transporter, *Science* 325 (2009) 1680–1682.
- [3] T.E. Wellems, *Plasmodium* chloroquine resistance and the search for a replacement antimalarial drug, *Science* 298 (2002) 124–126.
- [4] A.M. Dondrop, F. Nosten, W. Hanpithakpong, S.J. Lec, P. Ringwald, K. Silamut, M. Imwong, K. Chotivanich, P. Lim, T.A.S. Herdman, S. Yeung, P. Singhasivanon, N.P. Day, N. Linddegarth, D. Socheat, N.J. White, Artemisinin resistance in *Plasmodium falciparum* malaria, *N. Engl. J. Med.* 361 (2009) 455–467.
- [5] H. Noedl, D. Socheat, W. Satimal, Artemisinin-resistant malaria in Asia, *N. Engl. J. Med.* 361 (2009) 540–541.
- [6] R. Ettari, F. Bova, M. Zappala, S. Grasso, N. Micale, Falcipain-2 inhibitors, *Med. Res. Rev.* 30 (2010) 136–167.
- [7] M. Foley, L. Tilley, Quinoline antimalarial: mechanisms of action and resistance, *Int. J. Parasitol.* 27 (1997) 231–240.
- [8] J.X. Kelly, M.J. Smilkstein, R. Brun, W. Sergio, A.R. Cooper, K.D. Lane, A. Janowsky, R.A. Johnson, R.A. Dodean, R. Winter, D.J. Hinrichs, M.K. Riscoe, Discovery of dual function acridones as a new antimalarial chemotype, *Nature* 459 (2009) 270–273.
- [9] D. Mazier, L. Rénia, G. Snounou, A pre-emptive strike against malaria's stealthy hepatic forms, *Nat. Rev. Drug Discov.* 8 (2009) 855–864.
- [10] L. Adane, P.V. Bharatam, Modelling and informatics in the analysis of *P. falciparum* DHFR enzyme inhibitors, *Curr. Med. Chem.* 15 (2008) 1522–1569.
- [11] R.D. Powell, G.J. Brewer, Effects of pyrimethamine, chlorguanidine and primaquine against exoerythrocytic forms of a strain of chloroquine-resistant *Plasmodium falciparum* from Thailand, *Am. J. Trop. Med. Hyg.* 16 (1967) 693–698.
- [12] S. Vangapandu, S. Sachdeva, M. Jain, S. Singh, P. Singh, C.L. Kaul, R. Jain, 8-Quinolines and their pro-drug conjugates as potent blood-schizontocidal antimalarial agents, *Bioorg. Med. Chem.* 11 (2003) 4557–4568.
- [13] A. Agarwal, K. Srivastava, S.K. Puri, M.S. Chauhan, Synthesis of 4-pyrido-6-aryl-2-substituted amino pyrimidines as a new class of antimalarial agents, *Bioorg. Med. Chem.* 13 (2005) 6226–6232.
- [14] J. Wiesner, R. Ortmann, H. Jomaa, M. Schlitzer, New antimalarial drugs, *Angew. Chem. Int. Ed.* 42 (2003) 5274–5293.
- [15] C.E. Garrett, J.A. Coderre, T.D. Meek, E.P. Garvey, S.M. Beverly, D.V. Santi, A bifunctional thymidylate synthetase-dihydrofolate reductase in protozoa, *Mol. Biochem. Parasitol.* 11 (1984) 257–265.
- [16] V.F. Roche, Mechanism based inhibitors of deoxythymidine monophosphate synthesis as antineoplastic agents, *Am. J. Pharm. Educ.* 58 (1994) 196–203.
- [17] M.R. Hollingdale, P.P. McCann, A. Sjoerdsma, *Plasmodium berghei*: inhibitors of ornithine decarboxylase block exoerythrocytic schizogony, *Exp. Parasitol.* 60 (1985) 111–117.
- [18] G. Rastelli, W. Sirawaraporn, P. Sompornpisut, Interaction of pyrimethamine, cycloguanil, WR99210 and their analogues with *Plasmodium falciparum* dihydrofolate reductase: Structural basis of antifolate resistance, *Bioorg. Med. Chem.* 8 (2000) 1117–1128.
- [19] V. Kouznetsov, A. Gomez-Barrio, Recent developments in the design and synthesis of hybrid molecules based on aminoquinoline ring and their antiparasitological evaluation, *Eur. J. Med. Chem.* 44 (2009) 3091–3113.
- [20] P. Biginelli, Aldureids of ethylic acetoacetate and ethylic oxaloacetate, *Gazz. Chim. Ital* 23 (1893) 360–416.
- [21] K. Singh, K. Singh, An efficacious protocol for the oxidation of 3, 4-dihydropyrimidin-2(1H)-ones using pyridinium chlorochromate as catalyst, *Aust. J. Chem.* 61 (2008) 910–913.
- [22] K. Singh, K. Singh, B. Wan, S. Franzblau, K. Chibale, J. Balzarini, Facile transformation of 3,4-dihydropyrimidin-2(1H)-ones to pyrimidines in vitro evaluation as inhibitor of mycobacterium tuberculosis and modulators of cytostatic activity, *Eur. J. Med. Chem.* 46 (2011) 2290–2294.
- [23] N. October, N.D. Watermeyer, V. Yardley, T.J. Egan, K. Ncokazi, K. Chibale, Synthesis, antimalarial and cytotoxic evaluation of reversed chloroquinones based on the 3, 4-dihydropyrimidin-2(1H)-one scaffold, *Chem. Med. Chem.* 3 (2008) 1649–1653.
- [24] J.L. Vennerstrom, W.Y. Ellis, A.L. Ager, S.L. Anderaen Jr., L. Gerena, W.K. Milhous, N. N-Bis(7-chloroquinolin-4-yl) alkanediamines with potential against chloroquine-resistant malaria, *J. Med. Chem.* 35 (1992) 2129–2134.
- [25] F. Romanelli, K.M. Smith, A.D. Hoven, Chloroquine and hydroxychloroquine as inhibitors of human immunodeficiency virus (HIV-1) activity, *Curr. Pharm. Des.* 10 (2004) 2643–2648.
- [26] A. Savarino, J.R. Boelaert, A. Cassone, G. Majori, R. Cauda, Effects of chloroquine on viral infections: an old drug against today's diseases? *Lancet Infect. Dis.* 3 (2003) 722–727.
- [27] A. Dorn, S.R. Vippagunta, H. Matile, C. Jaquet, J.L. Vennerstrom, R.G. Ridley, An assessment of drug-haematin binding as a mechanism for inhibition of haematin polymerisation by quinoline antimalarials, *Biochem. Pharmacol.* 55 (1998) 727–736.
- [28] T.J. Egan, Interactions of quinoline antimalarials with haematin in solution, *J. Inorg. Biochem.* 100 (2006) 916–926.
- [29] T.J. Egan, K.K. Ncokazi, Quinoline antimalarials decrease the rate of beta-haematin formation, *J. Inorg. Biochem.* 99 (2005) 1532–1539.
- [30] A.C. Chou, R. Chevli, C.D. Fitch, Ferriprotoporphyrin IX fulfills the criteria for identification as the chloroquine receptor of malaria parasites, *Biochemistry* 19 (1980) 1543–1549.
- [31] T.J. Egan, W.W. Mavuso, D. Ross, H.M. Marques, Thermodynamic factor controlling the interaction of quinoline antimalarial drugs with ferriprotoporphyrin IX, *J. Inorg. Biochem.* 68 (1997) 137–145.
- [32] T.J. Egan, R. Hunter, C.H. Kaschula, H.M. Marques, A. Misplon, J. Walden, Structure-function relationships in aminoquinolines: effect of amino and chloro groups on quinoline-haematin complex formation, inhibition of β -haematin formation, and antiparasitological activity, *J. Med. Chem.* 43 (2000) 283–291.
- [33] K.C. Ingham, Application of jobs method of continuous variation to stoichiometry of protein-ligand complexes, *Anal. Biochem.* 68 (1975) 660–663.

- [34] C.Y. Huang, Determination of binding stoichiometry by the continuous variation method—the job plot, *Methods Enzymol.* 87 (1982) 509–525.
- [35] J.K. Natarajan, J.N. Alumasa, K. Yearick, K.A. Ekoue-Kovi, L.B. Casabianca, A.C.D. Dios, C. Wolf, P.D. Roepe, 4-N-, 4-S-, and 4-O-Chloroquine analogues: Influence of side chain length and quinolyl nitrogen pK_a on activity vs chloroquine resistant malaria, *J. Med. Chem.* 51 (2008) 3466–3479.
- [36] J.X. Kelly, R. Winter, M. Riscoe, D.H. Peyton, A spectroscopic investigation of the binding interaction between 4, 5-dihydroxyxanthone and heme, *J. Inorg. Biochem.* 86 (2001) 617–625.
- [37] F. Rodríguez, I. Rozas, M. Kaiser, R. Brun, B. Nguyen, W.D. Wilson, R.N. García, C. Dardonville, New Bis (2-aminoimidazoline) and bisguanidine DNA minor groove binders with potent in vivo antitrypanosomal and antiplasmodial activity, *J. Med. Chem.* 51 (2008) 909–923.
- [38] E. Deharo, R.N. Garcia, P. Oporto, A. Gimenez, M. Sauvain, V. Jullian, H. Ginsburg, A non-radiolabelled ferriprotoporphyrin IX biomineralisation inhibition test for the high throughput screening of antimalarial compounds, *Exp. Parasitol.* 100 (2002) 252–256.
- [39] F.S. Parker, J.L. Irvin, The interaction of chloroquine with nucleic acids and nucleoproteins, *J. Biol. Chem.* 199 (1952) 897–909.
- [40] P.H. Bolton, P.A. Mirau, R.H. Shafer, T.L. James, Interaction of the antimalarial drug fluoroquine with DNA, tRNA, and poly-(A): ¹⁹F-NMR chemical-shift and relaxation, optical absorption, and fluorescence studies, *Biopolymers* 20 (1981) 435–449.
- [41] J.L. Allison, R.L. O'Brien, F.E. Hahn, DNA: reaction with chloroquine, *Science* 149 (1965) 1111–1113.
- [42] N.B. Kurnick, I.E. Radcliffe, Reaction between DNA and quinacridine and other antimalarials, *J. Lab. Clin. Med.* 60 (1962) 669–688.
- [43] E.T. Mudasir, D.H. Wahyuni, N. Tjahjono, H. Yoshioka, Inoue, Spectroscopic studies on the thermodynamic and thermal denaturation of the CT-DNA binding of methylene blue, *Spectrochim. Acta Part A* 77 (2010) 528–534.
- [44] J. Cheng, R. Zeidan, S. Mishra, A. Liu, S.H. Pun, R.P. Kulkarni, G.S. Jensen, N.C. Belloq, M.E. Davis, Structure-function correlation of chloroquine and analogues as transgene expression enhancers in nonviral gene delivery, *J. Med. Chem.* 49 (2006) 6522–6531.
- [45] Y. Pollack, A.L. Katzen, D.T. Spira, J. Golenser, The genome of *Plasmodium falciparum* I: DNA base composition, *Nucleic Acids Res.* 10 (1982) 539–546.
- [46] F. Kwakye-Berko, S.R. Meshnick, Sequence preference of chloroquine binding to DNA and prevention of Z-DNA formation, *Mol. Biochem. Parasitol.* 39 (1990) 275–278.
- [47] J.M. Woynarowski, M. Krugliak, H. Ginsburg, Pharmacogenomic analyses of targeting the AT-rich malaria parasite genome with AT-specific alkylating drugs, *Mol. Biochem. Parasitol.* 154 (2007) 70–81.
- [48] H.A. Benesi, J.H. Hildebrand, A spectrophotometric investigation of the interaction of iodine with aromatic hydrocarbons, *J. Am. Chem. Soc.* 71 (1949) 2703–2707.
- [49] S.N. Cohen, K.L. Yielding, Spectrophotometric studies of the interaction of chloroquine with deoxyribonucleic acid, *J. Biol. Chem.* 240 (1965) 3123–3131.
- [50] N.I. Wenzel, N. Chavain, Y. Wang, W. Friebolin, L. Maes, B. Pradines, M. Lanzer, V. Yardley, R. Brun, C.H. Mende, C. Biot, K.T. Oth, E.D. Charvet, Antimalarial versus cytotoxic properties of dual drugs derived from 4-aminoquinolines and Mannich bases: interaction with DNA, *J. Med. Chem.* 53 (2010) 3214–3226.
- [51] R.E. Desjardins, C.J. Canfield, J.D. Haynes, J.D. Chulay, Quantitative assessment of antimalarial activity in vitro by a semiautomated microdilution technique, *Antimicrob. Agents Chemother.* 16 (1979) 710–718.
- [52] M. Rarey, B. Kramer, T.J. Lengauer, Multiple automatic base selection: protein-ligand docking based on incremental construction without manual intervention, *J. Comput. Aided Mol. Des* 11 (1997) 369–384.
- [53] M. Rarey, B. Kramer, T. Lengauer, G. Klebe, A fast flexible docking method using an incremental construction algorithm, *J. Mol. Biol.* 261 (1996) 470–489.
- [54] <http://www.tripos.com> (12.10.11).
- [55] J. Yuvaniyama, P. Chitnumsub, S. Kamchonwongpaisan, J. Vanichatanankul, W. Sirawaraporn, P. Taylor, Insights into antifolate resistance from malarial DHFR-TS structures, *Nat. Struct. Biol.* 10 (2003) 357–365.
- [56] L. Adane, P.V. Bharatam, V.J. Sharma, A common feature-based 3D-pharmacophore model generation and virtual screening: identification of potential *Pf*DHFR inhibitors, *Enz. Inhibit. Med. Chem.* 25 (2010) 635–645.